Structural Engineering and Mechanics, *Vol. 70, No. 5 (2019) 571-589*
DOI: https://doi.org/10.12989/sem.2019.70.5.571

Robust quasi 3D computational model for mechanical response of FG thick sandwich plate

Fatima Achouri[1,2], Samir Benyoucef*[2], Fouad Bourada[2,3], Rabbab Bachir Bouiadjra[1,2] and Abdelouahed Tounsi[2,4]

[1]*Department of Civil Engineering, University Mustapha Stambouli of Mascara, Algeria*
[2]*Material and Hydrology Laboratory, University of SidiBel Abbes, Faculty of Technology, Algeria*
[3]*Departement des Sciences et de la Technologie, Centre Universitaire de Tissemsilt, BP 38004 Ben Hamouda, Algeria*
[4]*Department of Civil and Environmental Engineering, King Fahd University of Petroleum & Minerals, 31261 Dhahran, Eastern Province, Saudi Arabia*

(Received January 21, 2019, Revised March 5, 2019, Accepted March 8, 2019)

Abstract. This paper aims to develop a quasi-3D shear deformation theory for the study of bending, buckling and free vibration responses of functionally graded (FG) sandwich thick plates. For that, in the present theory, both the components of normal deformation and shear strain are included. The displacement field of the proposed model contains undetermined integral terms and involves only four unknown functions with including stretching effect. Using Navier's technique the solution of the problem is derived for simply supported sandwich plate. Numerical results have been reported, and compared with those available in the open literature were excellent agreement was observed. Finally, a detailed parametric study is presented to demonstrate the effect of the different parameters on the flexural responses, free vibration and buckling of a simply supported sandwich plates.

Keywords: Quasi 3D solution; FG sandwich plate; bending; buckling; vibration; stretching effect

1. Introduction

FGMs are heterogeneous materials in which the properties vary from one surface to the other, continuously and gradually. The remarkable benefits offered by these materials compared to conventional materials and the demands for overcoming technical challenges have prompted an increased application of FGM structures (Ebrahimi and Reza Barati (2017)).

FGM plates are widely used in various engineering applications such as mechanical and civil engineering. These structures undergo different types of dynamic loads, bending and buckling. The analysis of these structures against these loads must be carried out to ensure safety and uninterrupted operation.

Sandwich structures are one of FGM plate type which have been the subject of more attention and are nowadays widely used in various types of engineering. This is due to its excellent advantages over the monolithic solid structure. FG Sandwich structures present improved characteristics such as higher stiffness and strength to weight ratio, long fatigue life and thermal resistances, etc. (Al-shujairi and Çağrı (2018)).

So far, many bending, buckling and vibration studies on FG structures such as plates, sandwich, beams and functionally graded-carbon nanotubes (FG-CNT) have been reported in several literatures (Ahmed 2014, Ait Amar *et al.* 2014, Akavci 2016, Kolahchi *et al.* 2016, Madani *et al.* 2016, Kolahchi *et al.* 2017a, Hajmohammad *et al.* 2017, Hosseini and Kolahchi 2018, Bourada *et al.* 2018 and 2019).

In order to study FG plate the classic plate theory (CPT) which neglected transverse shear stress and transverse normal stress was used. This theory gives good results for thin plates. Several researchers have used this theory in their research investigations such as (Kolahchi and Arani 2016, Bilouei *et al.* 2016, Zamanian *et al.* 2017).

Zenkour (2005a) and Zenkour and Alghamdi (2010) used the CPT for the study of the bending behavior of functionally graded sandwich plates.

Based on the CPT and nonlocal elasticity theory Shahsavari *et al*. (2017) studied the dynamic deflections of viscoelastic orthotropic nanoplates under moving load embedded within visco-Pasternak substrate and hygrothermal environment.

In the case of thick and moderately thick plates, the CPT gives inaccurate results. First order shear deformation (FSDT) proposed by Reissner (1945) and Mindlin (1951) includes the effect of transverse shear deformation. This theory has been widely used in several research publications such as (Kolahchi 2017, Zarei *et al.* 2017, Hajmohammad *et al.* 2018a, Amnieh *et al.* 2018)

Meksi *et al*. (2015) have analyzed the bending and free vibration of FG plate on elastic foundation by developing a new first-order shear deformation theory (NFSDT). Thai H.T. and Choi D.H. (2013) have developed a simple FSDT for the bending and free vibration analysis of functionally

*Corresponding author, Professor
E-mail: samir.benyoucef@gmail.com

ISSN: 1225-4568 (Print), 1598-6217 (Online)

graded plates. Also, Thai H.-T *et al*. (2014) developed a new FSDT for FG sandwich plates composed of FG face sheets and an isotropic homogeneous core. This theory has been developed in a way to eliminate the use of the shear correction factor. Karami *et al*. (2018a) studied the wave propagation in mounted nanoplates made of porous functionally graded materials by using the first-order shear deformation theory and nonlocal elasticity theory. Also, Karami and Janghorban (2019) used the Timoshenko beam model and the nonlocal strain gradient theory to study the vibration of porous nanotubes having thickness and material terms varying along the length. She Gui-Lin *et al*. (2018, 2019) presented an analytic model based on the nonlocal strain gradient theory for porous FG nanotubes to analyze the wave propagation and nonlinear bending behavior .

However, the FSDT depends on a shear correction factor which is difficult to estimate for composite materials. For this reason and to overcome this shortcoming, various higher order shear deformation theories (HSDT) have been developed.

Neves *et al*. (2012) have developed a hyperbolic theory counting for HSDT for static analysis of functionally graded sandwich plates. Nguyen *et al*. (2014) presented a trigonometric shear deformation theory to study the static, buckling and free vibration of two types of FG sandwich plates.

Karami *et al*. (2018b) presented a solution based on a second-order shear deformation theory in conjunction with nonlocal strain gradient theory for the wave propagation analysis of nanoplate made of temperature-dependent FG porous materials rested on Winkler–Pasternak foundation under in-plane magnetic field. Based on the same theory, Karami *et al*. (2018c) studied the thermal buckling of embedded sandwich piezoelectric nanoplates with functionally graded core.

Based on an n-order shear deformation theory, Xiang *et al*. (2011) presented a solution for free vibration of FG and composite sandwich plates. Also, using this theory and the meshless method, Xiang *et al*. (2013) analyzed the free vibration of FG sandwich plates. Alipour and Shariyat (2014) studied the stress and deformation analysis of functionally graded annular sandwich plates subjected to non-uniform normal and/or shear tractions. The high order shear deformation theory has also attracted the attention of other researchers (Kolahchi and Cheraghbak, 2017, Kolahchi 2017, Kolahchi *et al.* 2017b, Golabchi *et al.* 2018, Hajmohammad *et al.* 2018b, Petrov *et al.* 2018, Fakhar and Kolahchi 2018 and Hosseini and Kolahchi 2018).

These theories are cumbersome and costly in calculus due to involving many unknowns (Gupta and Talha (2017)).

Recently, new refined HSDT theories have been developed by researchers with low variables. Therefore, several works on FG sandwich plates have been developed on the basis of this theory (see references (Abdelaziz *et al.* 2011, Houari *et al.* 2011, Hadji *et al.* 2011, Merdaci *et al.* 2011, Bourada *et al.* 2012, Tounsi *et al.* 2013, Taibi *et al.* 2015, Li *et al.* 2016). Abdelaziz *et al*. (2017) presented a hyperbolic shear deformation theory for bending, buckling and vibration of PFG sandwich plate with various boundary conditions.

Shahsavari *et al*. (2018a) used the higher-order nonlocal strain-gradient model to analyze the vibration of single-layer graphene sheets (SLGSs) in hygrothermal environment. Thermal buckling behavior of FG porous nanobeam resting on Kerr foundation and integrated with piezoelectric has been investigated by Karami *et al*. (2018d). The nonlocal higher-order shear deformation beam theory was used. Karami *et al*. (2018 e) proposed a new size-dependent higher-order shear deformation theory for the wave dispersion in anisotropic doubly-curved nano shells. She *et al*. (2017) investigated the thermal buckling and post-buckling behavior of FG porous nanotubes using a refined beam theory. Karami *et al*. (2018f) used the refined HSDT to model the buckling behavior of FG nanoplate.

The two theories FSDT and HSDT are based on a key assumption which states that the transverse displacement through the thickness of the plate is constant. This led to neglecting the thickness stretching. However, this hypothesis is inadequate for thick plates (BachirBouiadjra *et al*. 2018)

Thus, needs exist for the development of quasi-3D HSDTs. In quasi 3D solutions, the stretching effect is naturally taken into account since the displacement is expanded as a higher-order variation through the thickness of the plate.

Mantari and Soares (2014) presented a solution including the thickness stretching effect with 5 unknown for the bending analysis of functionally graded single-layer and sandwich plates. Hamidi *et al*. (2015) investigate the thermomechanical bending response of functionally graded sandwich plates by using a theory with 5-unknowns and stretching effect. Bessaim *et al*. (2013) studied free vibration of functionally sandwich plates with FG face sheets based on higher-order shear and normal deformation theory with five unknown displacement functions. Hebali *et al*. (2014) proposed a new quasi-three-dimensional (3D) hyperbolic shear deformation theory for the bending and free vibration analysis of FGM plate. Mahmoudi *et al*. (2017) presented a refined 3D shear deformation theory for thermo-mechanical analysis of functionally graded sandwich plates resting on a Pasternak foundation.

Shahsavari *et al*. (2018b) presented a quasi-3D hyperbolic theory for the free vibration analysis of FG porous plates resting on different elastic foundations. Shahsavari *et al*. (2018c) used a new polynomial quasi-3D shear deformation theory in conjunction with the Eringen nonlocal differential model (ENDM) to study the size-dependent shear buckling force of FG materials.

Karami *et al*. (2018 g and h) develop a new size-dependent quasi-3D plate theory for the wave dispersion analysis of functionally graded nanoplates while resting on an elastic foundation and under the hygrothermal environment and for mechanical analysis of anisotropic nano-particles Also, Karami *et al*. (2019) present an accurate analysis of nanoshell structures by combining the HSDT with stretching effects and the Bi-Helmholtz non-local strain gradient elasticity theory (B-H-NSGT).

Recently, Tounsi and his co-workers (Meksi *et al*. (2019) Sekkal et *al*. (2017), Menasria *et al*. (2017), Bouhadra *et al*. (2018), Ait Sidhoum *et al*. (2017,2018), Bourada *et al*. (2016), Mahmoudi *et al*. (2018)) proposed a new displacement field which using undetermined integral terms. This new kinematic reduces the number of unknowns and equations of motion compared with other theories of the same nature.

This paper aims to improve this theory by including the stretching effect to study the bending, buckling, and free vibration of FG sandwich thick plate. The highlight of the proposed theory is that involves only four unknowns which is a reduced number of variables and governing equations than the conventional quasi-3D theories, but its solutions compare well with 3D and quasi-3D solutions.

In addition, it does not require a shear correction factor as in the case of FSDT and its scope is wider than the CPT since the CPT applies only to the case of thin plates. Equations of motion are obtained from Hamilton's principle. Analytical solutions of simply supported FG sandwich plates are presented. To check the validity of the present quasi 3D solution, the obtained results are compared with available data in literature. Parametric study is performed to show the influences many factors on the bending, buckling and free vibration of FGM sandwich plates.

2. Problem formulation

Consider a rectangular plate with length a, width b and uniform thickness h. The plate is assumed to be subjected to a transverse mechanical load at the top surface and a compressive in-plane load on the mid-plane of the plate. Three different types of FG plates are considered:

2.1 Type A: Isotropic FG plates

The plate of Type A is graded from metal at its bottom surface to ceramic at the top one (Fig. 1). The volume fraction of ceramic material *Vc* is given as follows is given as follows (Bourada *et al*. (2018), Attia *et al*. (2018), Bousahla *et al*. (2016)):

$$V_c = \left(\frac{2z+h}{2h}\right)^p \tag{1}$$

where p is the power-law index, which is positive and $z \in [-h/2, h/2]$.

2.2 Type B: Sandwich plates with FG core

The core of this type is graded from metal to ceramic. The bottom face is made of isotropic metal, whereas the top face is isotropic ceramic. The vertical positions of the bottom and top surfaces and of two interfaces between the layers are denoted by $h_0 = -h/2$, h_1, h_2, $h_3 = h/2$.respectively. h_1, h_2 vary according the thickness ratio of layers. The volume fraction functions of ceramic phase $V_c^{(j)}$ defined by Nguyen *et al*. (2014).

$$\begin{cases} V_c^{(j)}(z) = 0 & \text{for } z \in [h_0, h_1] \quad (2a) \\ V_c^{(j)}(z) = \left(\dfrac{z-h_1}{h_2-h_1}\right)^p & \text{for } z \in [h_1, h_2] \quad (2b) \\ V_c^{(j)}(z) = 1 & \text{for } z \in [h_2, h_3] \quad (2c) \end{cases}$$

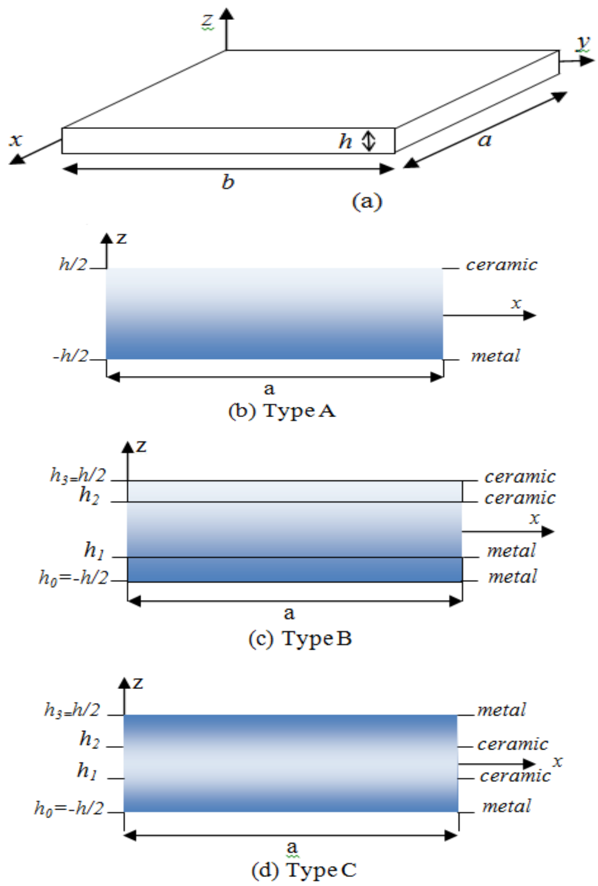

Fig. 1 Geometry of functionally graded plates

The variation of ceramic material through the plate thickness for (1-2-1) sandwich plate of Type B is displayed in fig. 1a.

2.3 Type C: Sandwich plates with FG faces

The faces of this type are graded from metal to ceramic. The core is made of isotropic ceramic. The volume fraction functions of ceramic phase $V_c^{(j)}$ given by (Nguyen *et al*. 2014):

$$\begin{cases} V_c^{(j)}(z) = \left(\dfrac{z-h_0}{h_1-h_0}\right)^p & \text{for } z \in [h_0, h_1] \quad (3a) \\ V_c^{(j)}(z) = 1 & \text{for } z \in [h_1, h_2] \quad (3b) \\ V_c^{(j)}(z) = \left(\dfrac{z-h_3}{h_2-h_3}\right)^p & \text{for } z \in [h_2, h_3] \quad (3c) \end{cases}$$

The variation of ceramic material through the plate thickness for (1-2-1) sandwich plate of Type C is displayed in Fig.1b.

2.4 Kinematics and strains

Based on a new inverse trigonometric shear deformation theory, the following displacement field is assumed (AitSidhoum *et al*. 2018):

$$u(x,y,z,t)=u_0(x,y,t)-z\frac{\partial w_0}{\partial x}+k_1\,f(z)\int\theta(x,y,t)\,dx \quad (4a)$$

$$v(x,y,z,t)=v_0(x,y,t)-z\frac{\partial w_0}{\partial y}+k_2\,f(z)\int\theta(x,y,t)\,dy \quad (4b)$$

$$w(x,y,z,t)=w_0(x,y,t)+g(z)\;\theta(x,y,t) \quad (4c)$$

Where $u_0;v_0;w_0;\theta$; are four unknown displacements of the mid-plane of the plate.

The coefficient k_1 *and* k_2 depends on the geometry. It can be seen that the kinematic in Eq. (4) introduces only four unknowns $(u, v_0, w_0\ and\ \theta)$ with considering the thickness stretching effect.

In this work, the present quasi – 3D HSDT is obtained by setting (Nguyen *et al*. 2014):

$$f(z)=h\arctan\left(\frac{rz}{h}\right)-\frac{16rz^3}{3h^2(r^2+4)} \quad (5)$$

The strain- displacement expressions, based on the formulation, are written under following compact form:

$$\begin{Bmatrix}\varepsilon_x\\ \varepsilon_y\\ \gamma_{xy}\end{Bmatrix}=\begin{Bmatrix}\varepsilon_x^0\\ \varepsilon_y^0\\ \gamma_{xy}^0\end{Bmatrix}+z\begin{Bmatrix}k_x^b\\ k_y^b\\ k_{xy}^b\end{Bmatrix}+f(z)\begin{Bmatrix}k_x^s\\ k_y^s\\ k_{xy}^s\end{Bmatrix} \quad (6)$$

$$\begin{Bmatrix}\gamma_{yz}\\ \gamma_{xz}\end{Bmatrix}=f'(z)\begin{Bmatrix}\gamma_{yz}^0\\ \gamma_{xz}^0\end{Bmatrix}+g(z)\begin{Bmatrix}\gamma_{yz}^1\\ \gamma_{xz}^1\end{Bmatrix}\quad \varepsilon_z=g'(z)\,\varepsilon_z^0$$

where

$$\begin{Bmatrix}\varepsilon_x^0\\ \varepsilon_y^0\\ \gamma_{xy}^0\end{Bmatrix}=\begin{Bmatrix}\dfrac{\partial u_0}{\partial x}\\ \dfrac{\partial v_0}{\partial x}\\ \dfrac{\partial u_0}{\partial y}+\dfrac{\partial v_0}{\partial x}\end{Bmatrix},\quad \begin{Bmatrix}k_x^b\\ k_y^b\\ k_{xy}^b\end{Bmatrix}=\begin{Bmatrix}-\dfrac{\partial^2 w_0}{\partial x^2}\\ -\dfrac{\partial^2 w_0}{\partial y^2}\\ -2\dfrac{\partial^2 w_0}{\partial x\partial y}\end{Bmatrix}, \quad (7a)$$

$$\begin{Bmatrix}k_x^s\\ k_y^s\\ k_{xy}^s\end{Bmatrix}=\begin{Bmatrix}k_1\theta\\ k_2\theta\\ k_1\dfrac{\partial}{\partial y}\int\theta\,dx+k_2\dfrac{\partial}{\partial x}\int\theta\,dy\end{Bmatrix},$$

$$g(z)=\frac{1}{9}\frac{\partial f(z)}{\partial z},\begin{Bmatrix}\gamma_{yz}^0\\ \gamma_{xz}^0\end{Bmatrix}=\begin{Bmatrix}k_2\int\theta\,dy\\ k_1\int\theta\,dx\end{Bmatrix},\quad \begin{Bmatrix}\gamma_{yz}^1\\ \gamma_{xz}^1\end{Bmatrix}=\begin{Bmatrix}\dfrac{\partial\theta}{\partial y}\\ \dfrac{\partial\theta}{\partial x}\end{Bmatrix}, \quad (7b)$$

$$\varepsilon_z^0=\theta \text{ and } \quad g'(z)=\frac{dg(z)}{dz}$$

The integrals presented in the above equations shall be resolved by a Navier type method and can be expressed as follows:

$$\frac{\partial}{\partial y}\int\theta\,dx=A'\frac{\partial^2\theta}{\partial x\partial y},\quad \frac{\partial}{\partial x}\int\theta\,dy=B'\frac{\partial^2\theta}{\partial x\partial y},$$
$$\int\theta\,dx=A'\frac{\partial\theta}{\partial x},\ \int\theta\,dy=B'\frac{\partial\theta}{\partial y} \quad (8)$$

Where the coefficients A' and B' are considered according to the type of solution employed, in this case via Navier method .Therefore, A', B', k_1 and k_2 are expressed as follows:

$$A'=-\frac{1}{\alpha^2},\quad B'=-\frac{1}{\beta^2},k_1=-\alpha^2,k_2=-\beta^2 \quad (9)$$

Where α and β are defined in expression 27.

The linear constitution relations are given below:

$$\begin{Bmatrix}\sigma_x\\ \sigma_y\\ \sigma_z\\ \tau_{xy}\\ \tau_{xz}\\ \tau_{yz}\end{Bmatrix}=\begin{bmatrix}C_{11}&C_{12}&C_{13}&0&0&0\\ C_{12}&C_{22}&C_{23}&0&0&0\\ C_{13}&C_{23}&C_{33}&0&0&0\\ 0&0&0&C_{66}&0&0\\ 0&0&0&0&C_{55}&0\\ 0&0&0&0&0&C_{44}\end{bmatrix}\begin{Bmatrix}\varepsilon_x\\ \varepsilon_y\\ \varepsilon_z\\ \gamma_{xy}\\ \gamma_{xz}\\ \gamma_{yz}\end{Bmatrix} \quad (10)$$

where C_{ij} are the three- dimensional elastic constants defined by:

$$C_{11}=C_{22}=C_{33}=\frac{(1-v)E(z)}{(1-2v)(1+v)}, \quad (11a)$$

$$C_{12}=C_{13}=C_{23}=\frac{vE(z)}{(1-2v)\,(1+2v)}, \quad (11b)$$

$$C_{44}=C_{55}=C_{66}=\frac{E(z)}{2(1+v)} \quad (11c)$$

2.5 Equation of motion

Hamilton's principle is herein employed to determine the equation of motion:

$$0=\int_0^t(\delta U+\delta V-\delta K)\,dt \quad (12)$$

Where δU is the variation of strain energy, δV is the variation of the external work done by external load applied to the place, and δK is the variation of kinetic energy.

The variation of strain energy of the plate is expressed by:

$$\delta U=\int_V\begin{bmatrix}\sigma_x\delta\,\varepsilon_x+\sigma_y\delta\,\varepsilon_y+\sigma_z\delta\,\varepsilon_z+\tau_{xy}\delta\,\gamma_{xy}\\ +\tau_{yz}\delta\,\gamma_{yz}+\tau_{xz}\delta\,\gamma_{xz}\end{bmatrix}dV$$
$$=\int_\Omega\begin{bmatrix}N_x\delta\,\varepsilon_x^0+N_y\delta\,\varepsilon_y^0+N_z\delta\,\varepsilon_z^0+N_{xy}\delta\,\gamma_{xy}^0\\ +M_x^b\delta\,k_x^b+M_y^b\delta\,k_y^b+M_{xy}^b\delta\,k_{xy}^b+M_x^s\delta\,k_x^s\\ +M_y^s\delta\,k_y^s+M_{xy}^s\delta\,k_{xy}^s+Q_{yz}^s\delta\,\gamma_{yz}^0+S_{yz}^s\delta\,\gamma_{yz}^1\\ +Q_{xz}^s\delta\,\gamma_{xz}^0+S_{xz}^s\delta\,\gamma_{xz}^1\end{bmatrix}dA \quad (13)$$

Where A is the top surface and the stress resultants N, M, S and Q are defined by

$$(N_i, M_i^b, M_i^s) = \int_{-h/2}^{h/2} (1, z, f)\ \sigma_i\ dz, \quad (i = x, y, xy);$$
$$N_z = \int_{-h/2}^{h/2} g'(z)\,\sigma_z\ dz \tag{14a}$$

$$(S_{xz}^s, S_{yz}^s) = \int_{-h/2}^{h/2} g(z)(\tau_{xz}, \tau_{yz})\, dz,$$
$$(Q_{xz}^s, Q_{yz}^s) = \int_{-h/2}^{h/2} f'(z)\,(\tau_{xz}, \tau_{yz})\, dz, \tag{14b}$$

The variation of work done by in – plane loads is given by:

$$\delta V = -\int_A \overline{N}\,\delta w\, dA - \int_A q\delta w\, dA \tag{15}$$

with

$$\overline{N} = \left[N_x^0 \frac{\partial^2 w}{\partial x^2} + 2\, N_{xy}^0 \frac{\partial^2 w}{\partial x \partial y} + N_y^0 \frac{\partial^2 w}{\partial y^2} \right] \tag{16}$$

Where (N_x^0, N_y^0, N_{xy}^0) are in – plane applied loads.

The variation of kinetic energy of the plate can be written as

$$\begin{aligned}
\delta K &= \int_V \left[\dot{u}\,\delta\,\dot{u} + \dot{v}\,\delta\,\dot{v} + \dot{w}\,\delta\,\dot{w} \right] \rho(z)\, dV \\
&= \int_A \Bigg\{ I_0 \left[\dot{u}_0 \delta \dot{u}_0 + \dot{v}_0 \delta \dot{v}_0 + \dot{w}_0 \delta \dot{w}_0 \right] - I_1 \left(\dot{u}_0 \frac{\partial \delta \dot{w}_0}{\partial x} + \frac{\partial \dot{w}_0}{\partial x} \delta\, \dot{u}_0 + \dot{v}_0 \frac{\partial \delta \dot{w}_0}{\partial y} + \frac{\partial \dot{w}_0}{\partial y} \delta\, \dot{v}_0 \right) \\
&+ J_1 \left((k_1 A') \left(\dot{u}_0 \frac{\partial \delta \dot{\theta}}{\partial x} + \frac{\partial \dot{\theta}}{\partial x} \delta\, \dot{u}_0 \right) + (k_2 B') \left(\dot{v}_0 \frac{\partial \delta \dot{\theta}}{\partial y} + \frac{\partial \dot{\theta}}{\partial y} \delta\, \dot{v}_0 \right) \right) \\
&+ J_1^{st} (\dot{w}_0 \delta \dot{\theta} + \dot{\theta} \delta \dot{w}_0) + I_2 \left(\frac{\partial \dot{w}_0}{\partial x} \frac{\partial \delta\, \dot{w}_0}{\partial x} + \frac{\partial \dot{w}_0}{\partial y} \frac{\partial \delta\, \dot{w}_0}{\partial y} \right) \\
&+ K_2 \left((k_1 A')^2 \left(\frac{\partial \dot{\theta}}{\partial x} \frac{\partial \delta\, \dot{\theta}}{\partial x} \right) + (k_2 B')^2 \left(\frac{\partial \dot{\theta}}{\partial y} \frac{\partial \delta\, \dot{\theta}}{\partial y} \right) \right) \\
&- J_2 \left(\begin{aligned} &(k_1 A') \left(\frac{\partial \dot{w}_0}{\partial x} \frac{\partial \delta\, \dot{\theta}}{\partial x} + \frac{\partial \dot{\theta}}{\partial x} \frac{\partial \delta\, \dot{w}_0}{\partial x} \right) + (k_2 B') \left(\frac{\partial \dot{w}_0}{\partial y} \frac{\partial \delta\, \dot{\theta}}{\partial y} + \frac{\partial \dot{\theta}}{\partial y} \frac{\partial \delta\, \dot{w}_0}{\partial y} \right) \\ &+ K_2^{st} \dot{\theta} \delta \dot{\theta} \end{aligned} \right) \Bigg\} dA
\end{aligned} \tag{17}$$

Where dot-superscript convention indicates the differentiation with respect to the time variable t; $\rho(z)$ is the mass density and (I_i, J_i, K_i) are mass inertias of metal and ceramic materials respectively expressed by:

$$(I_0, I_1, I_2) = \int_{-h/2}^{h/2} (1, z, z^2)\,\rho(z)\, dz \tag{18a}$$

$$(J_1, J_1^{st}, J_2, K_2, K_2^{st}) = \int_{-h/2}^{h/2} (f, g, zf, f^2, g^2)\,\rho(z)\, dz \tag{18b}$$

By substituting equations (13), (15) and (17) into equation (12), the following equation of motion can be obtained:

$$\begin{aligned}
\delta\, u_0 :\ & \frac{\partial N_x}{\partial x} + \frac{\partial N_{xy}}{\partial y} = I_0 \ddot{u}_0 - I_1 \frac{\partial \ddot{w}_0}{\partial x} + J_1 k_1 A' \frac{\partial \ddot{\theta}}{\partial x} \\
\delta\, v_0 :\ & \frac{\partial N_{xy}}{\partial x} + \frac{\partial N_y}{\partial y} = I_0 \ddot{v}_0 - I_1 \frac{\partial \ddot{w}_0}{\partial y} + J_1 k_2 B' \frac{\partial \ddot{\theta}}{\partial y} \\
\delta\, w_0 :\ & \frac{\partial^2 M_x^b}{\partial x^2} + 2 \frac{\partial^2 M_{xy}^b}{\partial x \partial y} + \frac{\partial^2 M_y^b}{\partial y^2} + N_x^0 \frac{\partial^2 w}{\partial x^2} \\
& + 2\, N_{xy}^0 \frac{\partial^2 w}{\partial x \partial y} + N_y^0 \frac{\partial^2 w}{\partial y^2} = I_0 \ddot{w}_0 + I_1 \left(\frac{\partial \ddot{u}_0}{\partial x} + \frac{\partial \ddot{v}_0}{\partial y} \right) \\
& + J_2 \left(k_1 A' \frac{\partial^2 \ddot{\theta}}{\partial x^2} + k_2 B' \frac{\partial^2 \ddot{\theta}}{\partial y^2} \right) - I_2 \nabla^2 \ddot{w}_0 + J_1^{ts} \ddot{\theta} \\
\delta\, \theta :\ & -k_1\, A' \frac{\partial^2 M_x^s}{\partial x^2} - k_2\, B' \frac{\partial^2 M_y^s}{\partial y^2} - (k_1 A' + k_2\, B') \frac{\partial^2 M_{xy}^s}{\partial x \partial y} \\
& + k_1\, A' \frac{\partial Q_{xz}}{\partial x} + k_2\, B' \frac{\partial Q_{yz}}{\partial y} - N_z + \frac{\partial S_{xz}^s}{\partial x} + \frac{\partial S_{yz}^s}{\partial y} \\
& + g(0) \left[N_x^0 \frac{\partial^2 w}{\partial x^2} + 2\, N_{xy}^0 \frac{\partial^2 w}{\partial x \partial y} + N_y^0 \frac{\partial^2 w}{\partial y^2} \right] = \\
& - J_1 \left(k_1 A' \frac{\partial \ddot{u}_0}{\partial x} + k_2 B' \frac{\partial \ddot{v}_0}{\partial y} \right) + J_2 \left(k_1 A' \frac{\partial^2 \ddot{w}_0}{\partial x^2} + k_2 B' \frac{\partial^2 \ddot{w}_0}{\partial y^2} \right) \\
& - K_2 \left((k_1 A')^2 \frac{\partial^2 \ddot{\theta}}{\partial x^2} + (k_2 B')^2 \frac{\partial^2 \ddot{\theta}}{\partial y^2} \right) + J_1^{st} \ddot{w}_0 + K_2^{st} \ddot{\theta}
\end{aligned} \tag{19}$$

The effective material properties at the j-th layer of FG plates according to the power-law form are expressed by:

$$P^{(j)}(z) = P_m + (P_c - P_m) V_c^{(j)}(z) \tag{20}$$

Where P_m and P_c are the Young's modulus (E), Poisson's ratio (ν), of metal and ceramic materials, respectively. For elastic and isotropic FG plates,

Substituting equation (7) into equation (10) and the subsequent results into equation (14), the stress resultants are obtained in terms of strains as following compact from:

$$\begin{Bmatrix} N \\ M^b \\ M^s \end{Bmatrix} = \begin{bmatrix} A & B & B^s \\ B & D & D^s \\ B^s & D^s & H^s \end{bmatrix} \begin{Bmatrix} \varepsilon \\ k^b \\ k^s \end{Bmatrix} + \varepsilon^0 \begin{Bmatrix} L \\ L^a \\ R \end{Bmatrix},$$
$$\begin{Bmatrix} Q \\ S \end{Bmatrix} = \begin{bmatrix} F^s & X^s \\ X^s & A^s \end{bmatrix} \begin{Bmatrix} \gamma^0 \\ \gamma^1 \end{Bmatrix} \tag{21a}$$

$$N_z = L(\varepsilon_x^0 + \varepsilon_y^0) + L^a (k_x^b + k_y^b) + R(k_x^s + k_y^s) + R^a \varepsilon_z^0 \tag{21b}$$

In which

$$\begin{aligned} N &= \{N_x, N_y, N_{xy}\}^t, \\ M^b &= \{M_x^b, M_y^b, M_{xy}^b\}^t, \\ M^s &= \{M_x^s, M_y^s, M_{xy}^s\}^t \end{aligned} \tag{22a}$$

$$\begin{aligned} \varepsilon &= \{\varepsilon_x^0, \varepsilon_y^0, \gamma_{xy}^0\}^t, \\ k^b &= \{k_x^b, k_y^b, k_{xy}^b\}^t, \\ k^s &= \{k_x^s, k_y^s, k_{xy}^s\}^t \end{aligned} \tag{22b}$$

$$A=\begin{bmatrix} A_{11} & A_{12} & 0 \\ A_{12} & A_{22} & 0 \\ 0 & 0 & A_{66} \end{bmatrix},\ B=\begin{bmatrix} B_{11} & B_{12} & 0 \\ B_{12} & B_{22} & 0 \\ 0 & 0 & B_{66} \end{bmatrix},\ D=\begin{bmatrix} D_{11} & D_{12} & 0 \\ D_{12} & D_{22} & 0 \\ 0 & 0 & D_{66} \end{bmatrix} \tag{22c}$$

$$B^s=\begin{bmatrix} B^s_{11} & B^s_{12} & 0 \\ B^s_{12} & B^s_{22} & 0 \\ 0 & 0 & B^s_{66} \end{bmatrix},\ D^s=\begin{bmatrix} D^s_{11} & D^s_{12} & 0 \\ D^s_{12} & D^s_{22} & 0 \\ 0 & 0 & D^s_{66} \end{bmatrix},\ H^s=\begin{bmatrix} H^s_{11} & H^s_{12} & 0 \\ H^s_{12} & H^s_{22} & 0 \\ 0 & 0 & H^s_{66} \end{bmatrix} \tag{22d}$$

$$\begin{gathered} Q=\left\{Q^s_{xz}, Q^s_{yz}\right\}^t,\ S=\left\{S^s_{xz}, S^s_{yz}\right\}^t, \\ \gamma^0=\left\{\gamma^0_{xz}, \gamma^0_{yz}\right\}^t,\ \gamma^1=\left\{\gamma^1_{xz}, \gamma^1_{yz}\right\}^t \end{gathered} \tag{22e}$$

$$F^s=\begin{bmatrix} F^s_{55} & 0 \\ 0 & F^s_{44} \end{bmatrix},\ X^s=\begin{bmatrix} X^s_{55} & 0 \\ 0 & X^s_{44} \end{bmatrix},\ A^s=\begin{bmatrix} A^s_{55} & 0 \\ 0 & A^s_{44} \end{bmatrix} \tag{22f}$$

$$\begin{Bmatrix} L \\ L^a \\ R \\ R^a \end{Bmatrix}=\int_z \lambda(z)\begin{Bmatrix} 1 \\ z \\ f(z) \\ g'(z)\dfrac{1-\nu}{\nu} \end{Bmatrix} g'(z)dz \tag{22g}$$

and stiffness components are given as:

$$\begin{Bmatrix} A_{11} & B_{11} & D_{11} & B^s_{11} & D^s_{11} & H^s_{11} \\ A_{12} & B_{12} & D_{12} & B^s_{12} & D^s_{12} & H^s_{12} \\ A_{66} & B_{66} & D_{66} & B^s_{66} & D^s_{66} & H^s_{66} \end{Bmatrix} = \int_z \lambda(z)(1, z, z^2, f(z), zf(z), f^2(z))\begin{Bmatrix} \dfrac{1-\nu}{\nu} \\ 1 \\ \dfrac{1-2\nu}{2\nu} \end{Bmatrix} dz \tag{23a}$$

$$\begin{gathered} (A_{22}, B_{22}, D_{22}, B^s_{22}, D^s_{22}, H^s_{22}) \\ =(A_{11}, B_{11}, D_{11}, B^s_{11}, D^s_{11}, H^s_{11}) \end{gathered} \tag{23b}$$

$$(F^s_{44}, X^s_{44}, A^s_{44}) = \int_{-h/2}^{h/2} \frac{E(z)}{2(1+\nu)}\left(\left[f'(z)\right]^2, f'(z)g(z), g^2(z)\right)dz \tag{23c}$$

$$(F^s_{55}, X^s_{55}, A^s_{55})=(F^s_{44}, X^s_{44}, A^s_{44}) \tag{23d}$$

By substituting equation (21) into equation (19), the equation of motion can be expressed in terms of displacements (u_0, v_0, w_0, θ) and the appropriate equations take the form:

$$\begin{aligned} & A_{11}d_{11}u_0 + A_{66}\, d_{22}u_0 + \left(A_{12}+A_{66}\right)d_{12}v_0 \\ & -B_{11}d_{111}w_0 - \left(B_{12}+2B_{66}\right)d_{122}w_0 \\ & +\left(B^s_{66}\left(k_1A'+k_2\,B'\right)+B^s_{12}k_2B'\right)d_{122}\theta \\ & +B^s_{11}k_1A'd_{111}\theta + Ld_1\theta = I_0\ddot{u}_0 - I_1d_1\ddot{w}_0 + J_1k_1A'd_1\ddot{\theta} \end{aligned} \tag{24a}$$

$$\begin{aligned} & A_{22}\,d_{22}v_0 + A_{66}\,d_{11}v_0 + \left(A_{12}+A_{66}\right)d_{12}u_0 \\ & -B_{22}\,d_{222}w_0 - \left(B_{12}+2B_{66}\right)d_{112}w_0 \\ & +\left(B^s_{66}\left(k_1A'+k_2\,B'\right)+B^s_{12}k_1A'\right)d_{112}\theta \\ & +B^s_{22}k_2B'd_{222}\theta + Ld_2\theta = I_0\ddot{v}_0 - I_1d_2\ddot{w}_0 \\ & +J_1k_2B'd_2\ddot{\theta} \end{aligned} \tag{24b}$$

$$\begin{aligned} & B_{11}\,d_{111}u_0 + \left(B_{12}+2B_{66}\right)d_{122}u_0 + \left(B_{12}+2B_{66}\right)d_{112}v_0 \\ & +B_{22}\,d_{222}v_0 - D_{11}d_{1111}w_0 - 2\left(D_{12}+2D_{66}\right)d_{1122}w_0 \\ & -D_{22}\,d_{2222}w_0 + D^s_{11}\,k_1A'\,d_{1111}\theta \\ & +\left((D^s_{12}+2D^s_{66})(k_1A'+k_2B')\right)d_{1122}\theta \\ & +D^s_{22}k_2B'\,d_{2222}\theta + L^a(d_{11}\theta + d_{22}\theta) \\ & +N^0_x d_{11}w + 2N^0_{xy}d_{12}w + N^0_y d_{22}w = \\ & I_0\ddot{w}_0 + I_1\left(d_1\ddot{u}_0 + d_2\ddot{v}_0\right) - I_2(d_{11}\ddot{w}_0 + d_{22}\ddot{w}_0) \\ & +J_2\left(k_1A'\,d_{11}\ddot{\theta} + k_2B'\,d_{22}\ddot{\theta}\right) + J^{ts}_1\ddot{\theta} \end{aligned} \tag{24c}$$

$$\begin{aligned} & -k_1A'\,B^s_{11}d_{111}u_0 - \left(B^s_{12}k_2B' + B^s_{66}\left(k_1A'+k_2B'\right)\right)d_{122}u_0 \\ & -\left(B^s_{12}k_1A' + B^s_{66}\left(k_1A'+k_2B'\right)\right)d_{112}v_0 - B^s_{22}k_2B'\,d_{222}v_0 \\ & +D^s_{11}k_1A'\,d_{1111}w_0\ \left((D^s_{12}+2D^s_{66})(k_1A'+k_2B')\right)d_{1122}w_0 \\ & +D^s_{22}k_2B'\,d_{2222}w_0 - H^s_{11}(k_1A')^2 d_{1111}\theta - H^s_{22}(k_2B')^2 d_{2222}\theta \\ & -\left(2H^s_{12}\,k_1\,k_2A'\,B' + (k_1A'+k_2B')^2\,H^s_{66}\right)d_{1122}\theta \\ & +\left((k_1A')^2F^s_{55} + 2k_1A'\,X^s_{55} + A^s_{55}\right)d_{11}\theta + \\ & \left((k_2B')^2F^s_{44} + 2k_2B'\,X^s_{44} + A^s_{44}\right)d_{22}\theta \\ & -2R(k_1A'\,d_{11}\theta + k_2B'\,d_{11}\theta) - L(d_1u_0 + d_2v_0) \\ & +L^a(d_{11}w_0 + d_{22}w_0) - R^a\theta + g(0)(N^0_x d_{11}w + \\ & 2N^0_{xy}d_{12}w + N^0_y d_{22}w) = -J_1\left(k_1A'\,d_1\ddot{u}_0 + k_2B'\,d_2\ddot{v}_0\right) \\ & +J_2(k_1A'\,d_{11}\ddot{w}_0 + k_2B'\,d_{22}\ddot{w}_0) \\ & -K_2\left((k_1A')^2 d_{11}\ddot{\theta} + (k_2B')^2 d_{22}\ddot{\theta}\right) + J^{st}_1\ddot{w}_0 + K^{st}_2\ddot{\theta} \end{aligned} \tag{24d}$$

where d_{ij}, d_{ijl} and d_{ijlm} are the following differential operators:

$$\begin{gathered} d_{ij}=\frac{\partial^2}{\partial x_i \partial x_j},\quad d_{ijl}=\frac{\partial^3}{\partial x_i \partial x_j \partial x_l},\quad d_{ijlm}=\frac{\partial^4}{\partial x_i \partial x_j \partial x_l \partial x_m}, \\ d_i=\frac{\partial}{\partial x_i},\ (i,j,l,m=1,2). \end{gathered} \tag{25}$$

2.6 Close form solutions

The Navier solution method is utilized to deduce the analytical solutions for which the displacement variables are written as product of arbitrary parameters and known trigonometric functions to respect the equation of motion and boundary condition.

$$\begin{Bmatrix} u_0 \\ v_0 \\ w_0 \\ \theta \end{Bmatrix}=\sum_{m=1}^{\infty}\sum_{n=1}^{\infty}\begin{Bmatrix} U_{mn}e^{i\omega t}\cos(\alpha\, x)\sin(\beta\, y) \\ V_{mn}e^{i\omega t}\sin(\alpha\, x)\cos(\beta\, y) \\ W_{mn}e^{i\omega t}\sin(\alpha\, x)\sin(\beta\, y) \\ X_{mn}e^{i\omega t}\sin(\alpha\, x)\sin(\beta\, y) \end{Bmatrix} \tag{26}$$

Where ω is the frequency of free vibration of the plate, $\sqrt{i}=-1$ the imaginary unit with

$$\alpha = m\pi / a \text{ and } \beta = n\pi / b \tag{27}$$

The transverse load q is also expanded in the double-Fourier sine series as:

$$q(x,y)=\sum_{m=1}^{\infty}\sum_{n=1}^{\infty} q_{mn}\sin(\alpha x)\sin(\beta y) \quad (28)$$

Where $q_{mn}=q_0$ forsinusoidally distributed load. Assuming that the plate is subjected to in-plane compressive loads of form: $N_x^0=-N_0$, $N_y^0=-\gamma N_0$, $N_{xy}^0=0$, $\gamma=N_y^0/N_x^0$ (whereγ are non – dimensional load parameter).

Substituting equations (26) and (28) into equation (24), the following equation is obtained:

$$\left(\begin{bmatrix} S_{11} & S_{12} & S_{13} & S_{15} \\ S_{12} & S_{22} & S_{23} & S_{24} \\ S_{13} & S_{23} & S_{33}+\eta & S_{34}+g(0)\eta \\ S_{14} & S_{24} & S_{34}+g(0)\eta & S_{44}+[g(0)]^2\eta \end{bmatrix} -\omega^2\begin{bmatrix} m_{11} & 0 & m_{13} & m_{14} \\ 0 & m_{22} & m_{23} & m_{24} \\ m_{13} & m_{23} & m_{33} & m_{34} \\ m_{14} & m_{24} & m_{34} & m_{44} \end{bmatrix}\right)\begin{Bmatrix} U_{mn} \\ Vmn \\ Wmn \\ Xmn \end{Bmatrix}=\begin{Bmatrix} 0 \\ 0 \\ q_{mn} \\ 0 \end{Bmatrix} \quad (29)$$

where

$$S_{11}=(\alpha^2 A_{11}+\beta^2 A_{66}),\ S_{12}=\alpha\beta(A_{12}+A_{66})$$
$$S_{13}=-\alpha^3 B_{11}-\alpha\beta^2(B_{12}+2B_{66})$$
$$S_{14}=\alpha((k_2B'B_{12}^s+(k_1A'+k_2B')B_{66}^s)\beta^2 +k_1A'B_{11}^s\alpha^2-L),\ S_{22}=(\alpha^2 A_{66}+\beta^2 A_{22})$$
$$S_{23}=-\alpha^2\beta(B_{12}+2B_{66})-\beta^3 B_{22}$$
$$S_{24}=\beta((k_1A'B_{12}^s+(k_1A'+k_2B')B_{66}^s)\alpha^2 +k_2B'B_{22}^s\beta^2-L)$$
$$S_{33}=(\alpha^4 D_{11}+\beta^4 D_{22}+2\alpha^2\beta^2(D_{12}+2D_{66})) \quad (30)$$
$$S_{34}=-(\alpha^4 k_1A'D_{11}^s+2\alpha^2\beta^2 k_2B'D_{12}^s+\beta^4 k_2B'D_{22}^s -2\alpha^2\beta^2(k_1A'+k_2B')D_{66}^s)+L^a(\alpha^2+\beta^2)$$
$$S_{44}=(k_1A'\alpha^4 H_{11}^s+\beta^4(k_2B')^2 H_{22}^s +(2k_1k_2A'B'H_{12}^s+(k_1A'+k_2B')^2 H_{66}^s)\alpha^2\beta^2 +\alpha^2((k_1A')^2F_{55}^s+2k_1A'X_{55}^s+A_{55}^s)+\beta^2((k_2B')^2F_{44}^s +2k_2B'X_{44}^s+A_{44}^s)-2R(k_1A'\alpha^2+k_2B'\beta^2)+R^a$$
$$\eta=-N_0(\alpha^2+\gamma\beta^2)$$

and

$$m_{11}=I_0,\ m_{13}=-\alpha I_1,\ m_{14}=J_1k_1A'\alpha,$$
$$m_{22}=I_0,\ m_{23}=-\beta I_1,\ m_{24}=k_2B'\beta J_1,$$
$$m_{33}=I_0+I_2(\alpha^2+\beta^2), \quad (30)$$
$$m_{34}=-J_2\left(k_1A'\alpha^2+k_2B'\beta^2\right)+J_1^s,$$
$$m_{44}=K_2\left((k_1A')^2\alpha^2+(k_2B')^2\beta^2\right)+K_2^{st}$$

Table 1 Material properties of metal and ceramic

Material	Young's modulus (GPa)	Mass density (kg/m^3)	Poisson's ratio
Aluminium (Al^*)	70	2702	0.3
Aluminium (Al)	70	2707	
Zirconia (ZrO_2)	151	3000	
Alumina (Al_2O_3)	380	3800	

Eq. (29) is a general form for bending, buckling and free vibration analysis of isotropic and FG sandwich plates under in-plane and transverse loads. In order to solve bending problem, the in plane compressive load N_0 and mass matrix M are set to zeros. The critical buckling loads (N_{cr}) can be obtained from the stability problem $|K_{ij}=0|$ while the free vibration problem is achieved by omitting both in-plane and transverse loads.

3. Numerical results and discussion

In this section, various numerical examples using the present quasi 3D solution are presented for bending, buckling and free vibration of simply supported FG sandwich plate. The results of the proposed computational solution will be first compared with existing data available in literature to check their accuracy. For this, the FGM sandwich plates are combined from ceramic and metal Al/ZrO_2 and Al/Al_2O_3 (see table 1 for their material properties). For convenience, the following dimensionless forms are used:

$$\bar{u}(z)=\frac{100h^3E_c}{a^4q_0}u\left(0,\frac{b}{2},z\right),\quad \bar{w}=\frac{10h^3E_c}{a^4q_0}w\left(\frac{a}{2},\frac{b}{2}\right),$$

$$\hat{w}=\frac{10h\ E_0}{a\ q_0}w\left(\frac{a}{2},\frac{b}{2}\right),\quad \bar{\sigma}_{xx}(z)=\frac{h}{a\ q_0}\sigma_{xx}\left(\frac{a}{2},\frac{b}{2},z\right),$$

$$\hat{\sigma}_{xx}(z)=\frac{10h^2}{a^2q_0}\sigma_{xx}\left(\frac{a}{2},\frac{b}{2},z\right),\quad \bar{\sigma}_{xy}(z)=\frac{h}{a\ q_0}\sigma_{xy}(0,0,z),$$

$$\bar{\sigma}_{xz}(z)=\frac{h}{a\ q_0}\sigma_{xz}\left(0,\frac{b}{2},z\right),\quad \bar{N}_{cr}=\frac{N_{cr}a^2}{E_{mh}^3},$$

$$\hat{N}_{cr}=\frac{N_{cr}a^2}{100\,E_0h^3},\quad \bar{\omega}=\frac{\omega ab}{\pi^2h}\sqrt{\frac{12(1-\nu_c^2)\rho_c}{E_c}}$$

$$\hat{\omega}=\frac{\omega a^2}{h}\sqrt{\frac{\rho_0}{E_0}},\quad \rho_0=1\,kg/m^3,\quad E_0=1\ GPa,$$

3.1 Bending analysis

In order to prove the validity of the present improved higher shear deformation theory, comparisons are made

Table 2 Comparison of the nondimensional stress and displacements of Al/Al_2O_3 square plates ($a/h=10$, Type A)

p	**Theory**	$\bar{u}(-h/4)$	$\bar{w}$	$\overline{\sigma_{xx}}(h/3)$	$\overline{\sigma_{xy}}(-h/3)$	$\overline{\sigma_{xz}}(h/6)$
1	present	0.6269	0.6110	1.5859	0.6013	0.3536
	HSDT (Nguyen *et al*. 2014)	0.6413	0.5890	1.4897	0.6111	0.2611
	Quasi-3D (Carrera *et al*. 2008)	0.6436	0.5875	1.5062	0.6081	0.2510
	Quasi-3D (Wu and Chui 2011)	0.6436	0.5876	1.5061	0.6112	0.2511
	SSDT (Zenkour 2006)	0.6626	0.5889	1.4894	0.6110	0.2622
	HSDT (Mantari *et al*. 2012)	0.6398	0.5880	1.4888	0.6109	0.2566
	TSDT (Thai and Kim 2013)	0.6414	0.5890	1.4898	0.6111	0.2608
2	present	0.8792	0.7874	1.4760	0.5362	0.3353
	HSDT (Nguyen *et al*. 2014)	0.8982	0.7573	1.3959	0.5442	0.2742
	Quasi-3D (Carrera *et al*. 2008)	0.9012	0.7570	1.4147	0.5421	0.2496
	Quasi-3D (Wu and Chui 2011)	0.9013	0.7571	1.4133	0.5436	0.2495
	SSDT (Zenkour 2006)	0.9281	0.7573	1.3954	0.5441	0.2763
	HSDT (Mantari *et al*. 2012)	0.8957	0.7564	1.3940	0.5438	0.2741
	TSDT (Thai and Kim 2013)	0.8984	0.7573	1.3960	0.5442	0.2737
4	present	1.0409	0.8402	1.2285	0.5657	0.2677
	HSDT (Nguyen *et al*. 2014)	1.0500	0.8816	1.1792	0.5669	0.2546
	Quasi-3D (Carrera *et al*. 2008)	1.0541	0.8823	1.1985	0.5666	0.2362
	Quasi-3D (Wu and Chui 2011)	1.0541	0.8823	1.1841	0.5671	0.2362
	SSDT (Zenkour 2006)	1.0941	0.8819	1.1783	0.5667	0.2580
	HSDT (Mantari *et al*. 2012)	1.0457	0.8814	1.1755	0.5662	0.2623
	TSDT (Thai and Kim 2013)	1.0502	0.8815	1.1794	0.5669	0.2537
8	present	1.0853	0.9411	0.9842	0.5945	0.2066
	HSDT (Nguyen *et al*. 2014)	1.0759	0.9746	0.9473	0.5857	0.2094
	Quasi-3D (Carrera *et al*. 2008)	1.0830	0.9738	0.9687	0.5879	0.2262
	Quasi-3D (Wu and Chui 2011)	1.0830	0.9739	0.9622	0.5883	0.2261
	SSDT (Zenkour 2006)	1.1340	0.9750	0.9466	0.5856	0.2121
	HSDT (Mantari *et al*. 2012)	1.0709	0.9737	0.9431	0.5850	0.2140
	TSDT (Thai and Kim 2013)	1.0763	0.9746	0.9477	0.5858	0.2088

between the results obtained from this theory and those of obtained by Nguyen *et al*. (2014), Carrera *et al*. (2008), Wu and Chui (2011), Zenkour (2006), Mantari *et al*. (2012) and Thai and Kim (2013), Zenkour (2006), Neves *et al*. (2013) and Bessaim *et al*. (2013).

As a first example, a square plate type A (Al/Al_2O_3) subjected to a sinusoidal load is studied. In table 2, displacement results, axials and transvers stress are compared with the HSDT of Nguyen *et al*. (2014), the quasi-three-dimensional (3D) solutions of Carrera *et al*. (2008) and Wu and Chui (2011), the sinusoidal shear deformation theory (SSDT) of Zenkour (2006), the HSDT of Mantari *et al*. (2012) and the third shear deformation theory (TSDT) of Thai and Kim (2013). It is clear that the results of the present quasi 3D solution are in very close agreement with the different shear deformation theories.

The second example is performed for the bending responses of a Al/Al_2O_3 square sandwich plate Type B. The results of the displacement and stresses are given for fifth values of the power index "*p*" as shown in Table 3. According to the results presented in this table it can be seen that the results of the present improved model are in very great agreement with those of the different solutions.

In the third example, a sandwich plate type C is examined. Table 4 shows the effects of power law index "p" on the dimensionless displacements and stresses for different configuration of the sandwich plate. The present results are compared with the results of the HSDT of Nguyen *et al*. (2014), the TSDT and the SSDT of Zenkour *et al*. (2005a), and the quasi 3D solutions of Zenkour *et al*. (2013), Neves *et al*. (2013) and Bessaim *et al*. (2013) respectively. It is clear from this table that whatever the case of the sandwich (2008) and Wu and Chui (2011), the sinusoidal shear deformation theory (SSDT) of Zenkour (2006), the HSDT of Mantari *et al*. (2012) and the third shear deformation theory (TSDT) of Thai and Kim (2013). It is clear that the results of the present quasi 3D solution are in very close agreement with the different shear deformation theories.

The second example is performed for the bending responses of a Al/Al_2O_3 square sandwich plate Type B. The results of the displacement and stresses are given for fifth

Table 3 Comparison of the nondimensional stress and displacements of Al/Al_2O_3 square sandwich plates ($a/h = 10$, Type B)

p	**Theory**	$\bar{u}(-h/4)$	$\bar{w}$	$\bar{\sigma}_{xx}(h/3)$	$\bar{\sigma}_{xy}(-h/3)$	$\bar{\sigma}_{xz}(h/6)$
0	Present	0.3033	0.3653	1.4906	0.9518	0.3050
	HSDT (Nguyen *et al*. 2014)	0.3247	0.3247	1.4761	1.0130	0.2161
	Quasi-3D (Neves *et al*. 2013)	-	0.3711	-	-	0.2227
0.5	Present	0.5002	0.5031	1.5677	0.6343	0.3402
	HSDT (Nguyen *et al*. 2014)	0.5542	0.5245	1.5750	0.6965	0.2509
	Quasi-3D (Neves *et al*. 2013)	-	0.5238	-	-	0.2581
1	Present	0.6532	0.6022	1.5451	0.4896	0.3429
	HSDT (Nguyen *et al*. 2014)	0.7337	0.6345	1.5691	0.5447	0.2733
	FSDT (Brischetto 2009)	-	0.6337	-	-	0.2458
	Quasi-3D (Carrera *et al*. 2011)	-	0.6324	-	-	0.2594
	Quasi-3D (Neves *et al*. 2012)	-	0.6305	-	-	0.2788
	Quasi-3D (Neves *et al*. 2013)	-	0.6305	-	-	0.2789
4	Present	0.9317	0.7811	1.1858	0.5013	0.2405
	HSDT (Nguyen *et al*. 2014)	1.0550	0.8331	1.2539	0.5614	0.2697
	FSDT (Brischetto 2009)	-	0.8191	-	-	0.1877
	Quasi-3D (Carrera *et al*. 2011)	-	0.8307	-	-	0.2398
	Quasi-3D (Neves *et al*. 2012)	-	0.8202	-	-	0.2778
	Quasi-3D (Neves *et al*. 2013)	-	0.8199	-	-	0.2747
10	Present	0.9618	0.8287	0.8679	0.5193	0.1524
	HSDT (Nguyen *et al*. 2014)	1.0798	0.8807	0.9258	0.5758	0.1982
	FSDT (Brischetto 2009)	-	0.8556	-	-	0.1234
	Quasi-3D (Carrera *et al*. 201□)	-	0.8740	-	-	0.1944
	Quasi-3D (Neves *et al*. 2012)	-	0.8650	-	-	0.2059
	Quasi-3D (Neves *et al*. 2013)	-	0.8645	-	-	0.2034

values of the power index "*p*" as shown in Table 3. According to the results presented in this table it can be seen that the results of the present improved model are in very great agreement with those of the different solutions. plate studied and whatever the value of the material index "*p*" the results of this model are in very good agreement with those of the literature.

Another comparison of the results of this method is presented in the following. Tables 5 presents the axial stress $\hat{\sigma}_{xx}$ of Al/ ZrO_2 sandwich plates type C for p = 0, 1, 2, 5 and10 and different sandwich configuration. As it can see from these tables, there is a good agreement between all solutions.

After these comparisons, it can be concluded that the present quasi 3D solution with only four unknowns is not only accurate but also efficient in predicting the bending responses of FG sandwich plates.

In figure 2, we present respectively the variations of transverse displacement and in-plane and out of plane stresses through the plate thickness of the FG plate type A with a/h=10 and different values of p.

From these figures, we can see that:

- The transverse displacement increases as the power law index p increases.

- For the axial non dimensional stress, we can see that this stress is tensile at the top surface and compressive at the bottom surface.

- The in-plane tangential stress is tensile at the bottom surface and compressive at the top surface of the FG plates. The distribution of the transverse shear stress through the thickness of the plate is not parabolic except the case of p=0 (isotropic plate).

Figures 3 and 4 plot respectively the variation of stresses through the thickness direction for different values of p of Al/Al_2O_3 and Al/ZrO_2 square sandwich plates subjected to sinusoidal load with $a/h = 10$ and for type B and Type C. As it can be seen from the case of sandwich plate type C (figure 4), the maximum stresses are situated at layer's interfaces except the case of sandwich plate 1-2-1 where the maximum is located at the mid plane.

3.2 Free vibration analysis

Other examples to check the accuracy of the present quasi 3D computational solution in predicting the natural frequency of FG plate and FG sandwich plate are reported in Tables 6, 7 and 8.

Table 6 gives a comparison of the non dimensional frequencies ϖ of a square FG plate type A between the present solution and those of Nguyen *et al*. (2014) and the 3D solution of Uymaz and Aydogdu (2007). It is observed an excellent agreement.

Table 7 compares the nondimensional fundamental frequency $(\hat{\omega})$ by the present theory for a square sandwich

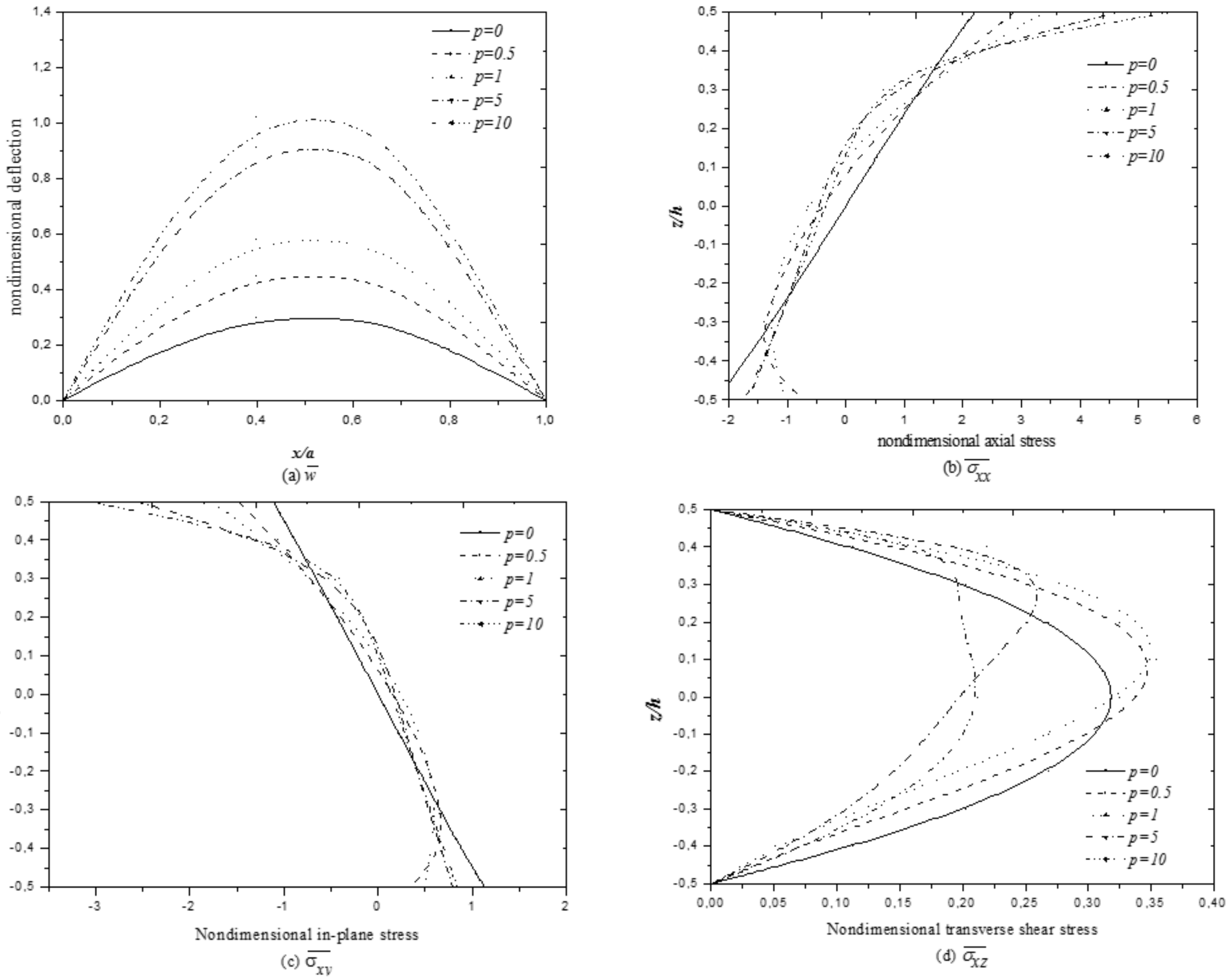

Fig. 2 Nondimensional displacements and stresses through the thickness direction for different values of p of Al/Al_2O_3 square plates subjected to sinusoidal load (a/h = 10, Type A)

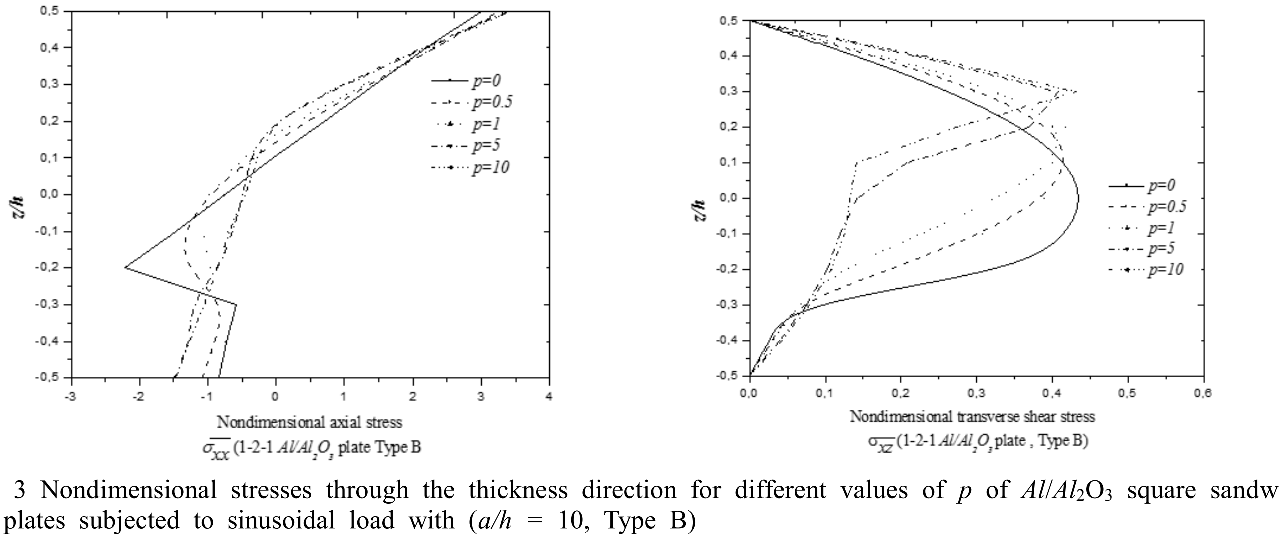

Fig. 3 Nondimensional stresses through the thickness direction for different values of p of Al/Al_2O_3 square sandw ich plates subjected to sinusoidal load with (a/h = 10, Type B)

plates (Al/Al_2O_3, type B) with those given by Nguyen *et al.* (2014) and the two HSDT given by Natarajan and Manickam (2012). The results are given for three value of the ratio a / h and three configuration of the sandwich plate. From the results shown in the table, there is a slight difference. This can be explained by the fact that HSDTs neglect the effect of stretching thing that is taken into consideration by the present 3D solution.

The nondimensional fundamental frequency $\hat{\omega}$ for a rectangular FG sandwich plates Al/Al_2O_3 type C predicted

Table 4 Nondimensional center deflections ($\hat{w}$) of Al/Zr_2O_2 square sandwich plates (a/h = 10, Type C)

p	**Theory**	**1-0-1**	**2-1-2**	**2-1-1**	**1-1-1**	**2-2-1**	**1-2-1**
	Present	0.19344	0.19344	0.19344	0.19344	0.□9344	0.19344
	HSDT (Nguyen *et al*. 2014)	0.19597	0.19597	0.19597	0.19597	0.19597	0.19597
	TSDT (Zenkour 2005a)	0.19606	0.19606	–	0.19606	0.19606	0.19606
0	SSDT (Zenkour 2005a)	0.19605	0.19605	–	0.19605	0.19605	0.19605
	Quasi-3D (Zenkour 2013)	0.19487	0.19487	–	0.19487	0.19487	0.19487
	Quasi-3D (Neves *et al*. 2013)	–	0.19490	0.19490	0.19490	0.19490	0.19490
	Quasi-3D (Bessaim *et al*. 2013)	–	0.19486	0.19486	0.19486	0.19486	0.19486
	Present	0.31463	0.29750	0.28854	0.28377	0.27331	0.26394
	HSDT (Nguyen *et al*. 2014)	0.32348	0.30622	0.29666	0.29191	0.28077	0.27086
	TSDT (Zenkour 2005a)	0.32358	0.30632	–	0.29199	0.28085	0.27094
1	SSDT (Zenkour 2005a)	0.32349	0.30624	–	0.29194	0.28082	0.27093
	Quasi-3D (Zenkour 2013)	0.32001	0.30275	–	0.28867	0.27760	0.26815
	Quasi-3D (Neves *et al*. 2013)	–	0.30700	0.29750	0.29290	0.28200	0.27220
	Quasi-3D (Bessaim *et al*. 2013)	–	0.30430	0.29448	0.29007	0.27874	0.26915
	Present	0.36232	0.34055	0.32699	0.32174	0.30610	0.29330
	HSDT (Nguyen *et al*. 2014)	0.37322	0.35221	0.33769	0.33279	0.31608	0.30255
	TSDT (Zenkour 2005a)	0.37335	0.35231	–	0.33289	0.31617	0.30263
2	SSDT (Zenkour 2005a)	0.37319	0.35218	–	0.33280	0.31611	0.30260
	Quasi-3D (Zenkour 2013)	0.36891	0.34737	–	0.32816	0.31152	0.29874
	Quasi-3D (Neves *et al*. 2013)	–	0.35190	0.33760	0.33290	0.31640	0.30320
	Quasi-3D (Bessaim *et al*. 2013)	–	0.35001	0.33495	0.33068	0.31356	0.30060
	Present	0.39895	0.37827	0.36072	0.35769	0.33724	0.32296
	HSDT (Nguyen *et al*. 2014)	0.40911	0.39170	0.37295	0.37134	0.34950	0.33472
	TSDT (Zenkour 2005a)	0.40927	0.39183	–	0.37145	0.34960	0.33480
5	SSDT (Zenkour 2005a)	0.40905	0.39160	–	0.37128	0.34950	0.33474
	Quasi-3D (Zenkour 2013)	0.40532	0.38612	–	0.36546	0.34361	0.32966
	Quasi-3D (Neves *et al*. 2013)	–	0.39050	0.37220	0.37050	0.34900	0.33470
	Quasi-3D (Bessaim *et al*. 2013)	–	0.38934	0.36981	0.36902	0.34649	0.33255
	Present	0.40915	0.39069	0.37218	0.37110	0.34911	0.33538
	HSDT (Nguyen *et al*. 2014)	0.41754	0.40393	0.3843	0.38540	0.36202	0.34815
	TSDT (Zenkour 2005a)	0.41772	0.40407	–	0.38551	0.36215	0.34824
10	SSDT (Zenkour 2005a)	0.41750	0.40376	–	0.38490	0.34916	0.34119
	Quasi-3D (Zenkour 2013)	0.41448	0.39856	–	0.37924	0.35577	0.34259
	Quasi-3D (Neves *et al*. 2013)	–	0.40260	0.38350	0.38430	0.36120	0.34800
	Quasi-3D (Bessaim *et al*. 2013)	–	0.40153	0.38111	0.38303	0.35885	0.34591

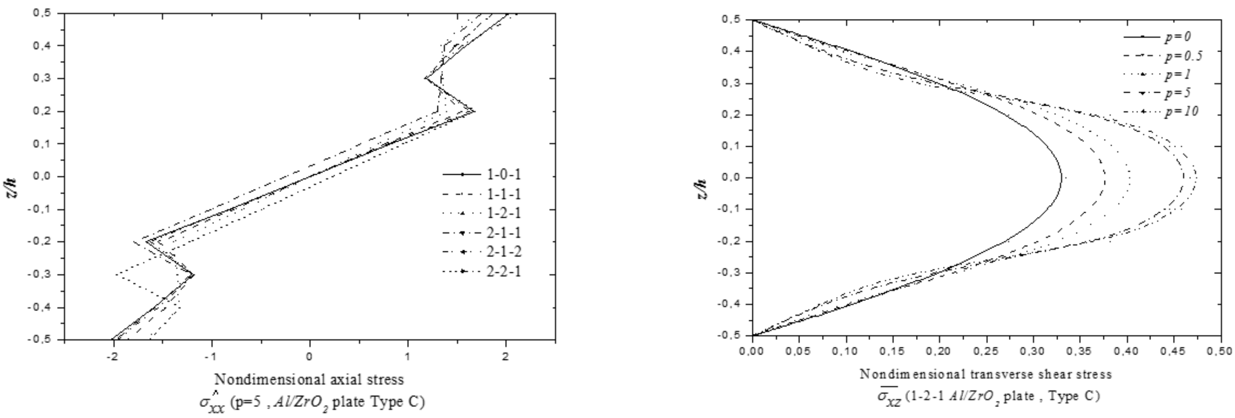

Fig. 4 Nondimensional stresses through the thickness direction for different values of p of Al/ZrO_2 square sandwich plates subjected to sinusoidal load with ($a/h=10$,Type C)

Table 5 Nondimensional axial stress $\hat{\sigma}_{xx}(h/2)$ of Al/Zr_2O_2 square sandwich plates(a/h = 10, Type C)

p	Theory	1-0-1	2-1-2	2-1-1	1-1-1	2-2-1	1-2-1
0	present	2.05448	2.05448	2.05448	2.05448	2.05448	2.05448
	HSDT (Nguyen *et al*. 2014)	1.99482	1.99482	1.99482	1.99482	1.99482	1.99482
	TSDT (Zenkour 2005a)	2.04985	2.04985	–	2.04985	2.04985	2.04985
	SSDT (Zenkour 2005a)	2.05452	2.05452	–	2.05452	2.05452	2.05452
	Quasi-3D (Zenkour 2013)	2.00773	2.00773	–	2.00773	2.00773	2.00773
	Quasi-3D (Neves *et al*. 2013)	–	2.00660	2.00640	2.00660	2.00650	2.00640
	Quasi-3D (Bessaim *et al*. 2013)	–	1.99524	1.99524	1.99524	1.99524	1.99524
1	present	1.60902	1.52551	1.41084	1.45341	1.33931	1.34511
	HSDT (Nguyen *et al*. 2014)	1.54441	1.46297	1.35703	1.39406	1.28852	1.29174
	TSDT (Zenkour 2005a)	1.57923	1.49587	–	1.42617	1.32062	1.32309
	SSDT (Zenkour 2005a)	1.58204	1.49859	–	1.42892	1.32342	1.32590
	Quasi-3D (Zenkour 2013)	1.57004	1.48833	–	1.41781	1.30907	1.31204
	Quasi-3D (Neves *et al*. 2013)	–	1.48130	1.37680	1.41370	1.30920	1.31330
	Quasi-3D (Bessaim *et al*. 2013)	–	1.46131	1.35053	1.39243	1.28274	1.29030
2	present	1.85971	1.76303	1.59352	1.66669	1.49720	1.51163
	HSDT (Nguyen *et al*. 2014)	1.78383	1.68682	1.52988	1.59393	1.43693	1.44707
	TSDT (Zenkour 2005a)	1.82167	1.72144	–	1.62748	1.47095	1.47988
	SSDT (Zenkour 2005a)	1.82450	1.72412	–	1.63025	1.47387	1.48283
	Quasi-3D (Zenkour 2013)	1.81509	1.72030	–	1.62591	1.46372	1.47421
	Quasi-3D (Neves *et al*. 2013)	–	1.69940	1.54560	1.60880	1.45430	1.46590
	Quasi-3D (Bessaim *et al*. 2013)	–	1.68472	1.52101	1.59170	1.42887	1.44497
5	present	2.02673	1.96180	1.74878	1.86542	1.64438	1.68005
	HSDT (Nguyen *et al*. 2014)	1.95031	1.87709	1.67895	1.78159	1.57620	1.60459
	TSDT (Zenkour 2005a)	1.99272	1.91302	–	1.81580	1.61181	1.63814
	SSDT (Zenkour 2005a)	1.99567	1.91547	–	1.81838	1.61477	1.64106
	Quasi-3D (Zenkour 2013)	1.97912	1.91504	–	1.82018	1.60953	1.63906
	Quasi-3D (Neves *et al*. 2013)	–	1.88380	1.69090	1.79060	1.58930	1.61950
	Quasi-3D (Bessaim *et al*. 2013)	–	1.87516	1.66856	1.77919	1.56627	1.60203
10	present	2.05479	2.01933	1.79924	1.93603	1.69875	1.74982
	HSDT (Nguyen *et al*. 2014)	1.98382	1.93431	1.72890	1.84933	1.62840	1.67019
	TSDT (Zenkour 2005a)	2.03036	1.97126	–	1.88376	1.66660	1.70417
	SSDT (Zenkour 2005a)	2.03360	1.97313	–	1.88147	1.61979	1.64851
	Quasi-3D (Zenkour 2013)	2.00692	1.97075	–	1.89162	2.18558	1.67350
	Quasi-3D (Neves *et al*. 2013)	–	1.93970	1.74050	1.85590	1.63950	1.68320
	Quasi-3D (Bessaim *et al*. 2013)	–	1.93266	1.71835	1.84705	1.61792	1.66754

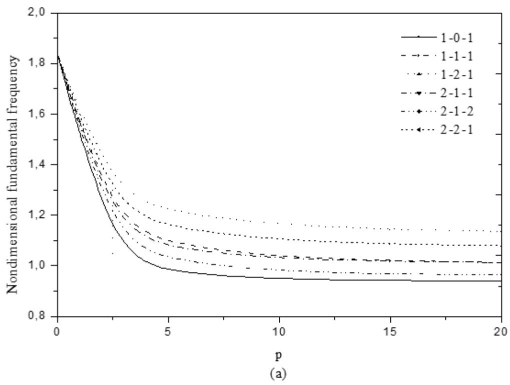

Fig. 5 Effect of the power-law index p on the nondimensional fundamental frequency ($\hat{\omega}$) of Al/Al_2O_3 square sandwich plates (a/h = 10, Type C)

by Nguyen *et al*. (2014) using the HSDT, Zenkour (2005b) using the TSDT and SSDT, Bessaim *et al*. (2013) using a quasi 3D solution, Li *et al*. (2008) using a 3D modeland the present theory are compared in Table 8. An excellent agreement is observed.

Figure 5 plots the variation of the non-dimensional fundamental natural frequency of simply supported FG sandwich plate type C as a function the power-law index.

As can be seen, the increase in the power index p reduces the frequency. On the other hand, the lowest frequencies and the largest correspond respectively to sandwich plates type 1-0-1 and 1-2-1. On the other hand, the lowest frequencies and the largest correspond respectively to sandwich plates type 1-0-1 and 1-2-1 this is due to the fact that these plates contain the lowest and the largest volume fraction of the ceramic. The latter plays a very important role in making the plate flexible or rigid.

Table 6 Comparison of the nondimensional fundamental frequency ϖ of Al^{*}/ZrO_2 square plates (Type A)

a/h	**Theory**	**power - law index**							
		0	0.1	0.2	0.5	1	2	5	10
2	present	1.2671	1.2383	1.2134	1.1570	1.0998	1.0425	0.9840	0.9580
	HSDT (Nguyen *et al*. 2014)	1.2454	1.2162	1.1913	1.1356	1.0784	1.0234	0.9685	0.9435
	3D (Uymaz and Aydogdu 2007)	1.2589	1.2296	1.2049	1.1484	1.0913	1.0344	0.9777	0.9507
5	present	1.7830	1.7369	1.6982	1.6149	1.5392	1.4762	1.4175	1.3786
	HSDT (Nguyen *et al*. 2014)	1.7683	1.7208	1.6818	1.5974	1.5212	1.4601	1.4058	1.3690
	3D (Uymaz and Aydogdu 2007)	1.7748	1.7262	1.6881	1.6031	1.4764	1.4628	1.4106	1.3711
10	present	1.9388	1.8861	1.8424	1.7503	1.6708	1.6108	1.5575	1.5139
	HSDT (Nguyen *et al*. 2014)	1.9317	1.8773	1.8332	1.7393	1.6583	1.5986	1.5492	1.5083
	3D (Uymaz and Aydogdu 2007)	1.9339	1.8788	1.8357	1.7406	1.6583	1.5968	1.5491	1.5066
20	present	1.9853	1.9303	1.8849	1.7902	1.7100	1.6520	1.6012	1.5561
	HSDT (Nguyen *et al*. 2014)	1.9821	1.9254	1.8797	1.7827	1.7003	1.6415	1.5943	1.5521
	3D (Uymaz and Aydogdu 2007)	1.9570	1.9261	1.8788	1.7827	1.6999	1.6401	1.5937	1.5491
50	present	1.9989	1.9431	1.8972	1.8017	1.7215	1.6642	1.6143	1.5687
	HSDT (Nguyen *et al*. 2014)	1.9971	1.9397	1.8935	1.7956	1.7129	1.6543	1.6078	1.5652
	3D (Uymaz and Aydogdu 2007)	1.9974	1.9390	1.8920	1.7944	1.7117	1.6522	1.6062	1.5620
100	present	2.0009	1.9450	1.8990	1.8033	1.7231	1.6659	1.6162	1.5705
	HSDT (Nguyen *et al*. 2014)	1.9993	1.9418	1.8955	1.7975	1.7147	1.6562	1.6098	1.5671
	3D (Uymaz and Aydogdu 2007)	1.9974	1.9418	1.8920	1.7972	1.7117	1.6552	1.6062	1.5652

Table 7 Comparison of the nondimensional fundamental frequency $(\hat{\omega})$ of Al/Al_2O_3 square sandwich plates (Type B)

a/h	**Theory**	**1-1-1**				**1-2-1**			**2-2-1**		
		0	0.5	1	5	0.5	1	5	0.5	1	5
5	present	1.2985	1.2412	1.2121	1.1635	1.2818	1.2326	1.1545	1.2022	1.1791	1.1383
	HSDT (Nguyen *et al*. 2014)	1.1147	1.1414	1.1561	1.1996	1.1574	1.1827	1.2569	1.1916	1.2268	1.3160
	HSDT (Natarajan and Manickam 2012)	1.1021	1.1449	1.1639	1.2113	1.1597	1.1884	1.2644	1.1965	1.2350	1.3249
	HSDT(Natarajan and Manickam 2012)	1.0893	1.1511	1.1701	1.2162	1.1663	1.1952	1.2712	1.2031	1.2421	1.3312
10	present	1.3744	1.3217	1.2964	1.2625	1.3665	1.3209	1.2650	1.2895	1.2757	1.2638
	HSDT (Nguyen *et al*. 2014)	1.2172	1.2359	1.2478	1.2883	1.2567	1.2763	1.3466	1.2827	1.3187	1.4130
	HSDT (Natarajan and Manickam 2012)	1.2138	1.2373	1.2506	1.2921	1.2578	1.2785	1.3492	1.2846	1.3216	1.4161
	HSDT (Natarajan and Manickam 2012)	1.2087	1.2392	1.2524	1.2935	1.2598	1.2806	1.3513	1.2865	1.3238	1.4180
100	present	1.3934	1.3482	1.3269	1.3030	1.3937	1.3529	1.3114	1.3221	1.3144	1.3174
	HSDT (Nguyen *et al*. 2014)	1.2617	1.2752	1.2853	1.3238	1.2984	1.3147	1.3824	1.3198	1.3558	1.4518
	HSDT (Natarajan and Manickam 2012)	1.2617	1.2751	1.2854	1.3239	1.2981	1.3148	1.3825	1.3198	1.3559	1.4519
	HSDT (Natarajan and Manickam 2012)	1.2616	1.2751	1.2854	1.3239	1.2981	1.3148	1.3825	1.3198	1.3559	1.4519

3.3 Buckling analysis

First, for the verification purpose, the results computed by the present quasi 3D theory are compared with those obtained by different higher shear deformation theory as reported in tables 9 and 10.

In table 9, we present a comparison of the critical buckling load of FG plate "type A" obtained from the present solution and those of Nguyen *et al*. (2014) and Thai and Choi (2012). The results are presented for different power law index "p" and different ratio of a/h and a/b. Also, two cases are studied plate subjected to uniaxial compression $\gamma = 0$ and biaxial compression $\gamma = 1$. It can be seen from this table that there is an excellent agreement between the results.

Another comparison is presented in Table 10. Critical buckling loads are obtained for sandwich plate "type B" and for biaxial compressive loads. The comparison with the different theories and for the different scheme of sandwich plates reveals that the results of the present theory are in very great concordance.

Table 11 gives the critical buckling loads of Al/Al_2O_3 square sandwich plate type B under biaxial compressions. Three scheme of sandwich plate are presented 1-1-1, 1-2-1 and 2-2-1.

Table 8 Nondimensional fundamental frequency ($\hat{\omega}$) of Al/Al_2O_3 square sandwich plates(a/h = 10,Type C)

p	**Theory**	**1-0-1**	**2-1-2**	**2-1-1**	**1-1-1**	**2-2-1**	**1-2-1**
0	present	1.83452	1.83452	1.83452	1.83452	1.83452	1.83452
	HSDT (Nguyen *et al*. 2014)	1.82489	1.82489	1.82489	1.82489	1.82489	1.82489
	TSDT (Zenkour 2005b)	1.82445	1.82445	1.82445	1.82445	1.82445	1.82445
	SSDT (Zenkour 2005b)	1.82452	1.82452	1.82452	1.82452	1.82452	1.82452
	Quasi-3D (Bessaim *et al*. 2013)	1.82682	1.82682	–	1.82682	1.82682	1.82682
	3D (Li *et al*. 2008)	1.82682	1.82682	–	1.82682	1.82682	1.82682
0.5	present	1.46638	1.50645	1.52819	1.54086	1.56800	1.59425
	HSDT (Nguyen *et al*. 2014)	1.44348	1.48355	1.50597	1.51885	1.54680	1.57437
	TSDT (Zenkour 2005b)	1.44424	1.48408	1.51253	1.51922	1.55199	1.57451
	SSDT (Zenkour 2005b)	1.44436	1.48418	1.51258	1.51927	1.55202	1.57450
	Quasi-3D (Bessaim *et al*. 2013)	1.44621	1.48611	–	1.52130	1.55016	1.57670
	3D (Li *et al*. 2008)	1.44614	1.48608	–	1.52131	1.54926	1.57668
1	present	1.27115	1.32941	1.36216	1.38183	1.42324	1.46496
	HSDT (Nguyen *et al*. 2014)	1.24332	1.30024	1.33352	1.35345	1.39579	1.43948
	TSDT (Zenkour 2005b)	1.24320	1.30011	1.34888	1.35333	1.40789	1.43934
	SSDT (Zenkour 2005b)	1.24335	1.30023	1.34894	1.35339	1.40792	1.43931
	Quasi-3D (Bessaim *et al*. 2013)	1.24495	1.30195	–	1.35527	1.39987	1.44143
	3D (Li *et al*. 2008)	1.24470	1.30181	–	1.35523	1.39763	1.44137
5	present	0.97167	1.01844	1.06756	1.08337	1.14760	1.21055
	HSDT (Nguyen *et al*. 2014)	0.94611	0.98193	1.03067	1.04473	1.10905	1.17403
	TSDT (Zenkour 2005b)	0.94598	0.98184	1.07432	1.04466	1.14731	1.17397
	SSDT (Zenkour 2005b)	0.94630	0.98207	1.07445	1.04481	1.14741	1.17399
	Quasi-3D (Bessaim *et al*. 2013)	0.94716	0.98311	–	1.04613	1.11723	1.17579
	3D (Li *et al*. 2008)	0.94476	0.98103	–	1.04532	1.10983	1.17567
10	present	0.94693	0.97831	1.02814	1.03476	1.10038	1.16140
	HSDT (Nguyen *et al*. 2014)	0.92854	0.94305	0.99219	0.99558	1.06114	1.12320
	TSDT (Zenkour 2005b)	0.92839	0.94297	1.03862	0.99551	1.10533	1.12314
	SSDT (Zenkour 2005b)	0.92875	0.94332	1.04558	0.99519	1.04154	1.13460
	Quasi-3D (Bessaim *et al*. 2013)	0.92952	0.94410	–	0.99684	1.07015	1.12486
	3D (Li *et al*. 2008)	0.92727	0.94078	–	0.99684	1.06104	1.12466

Table 9 Comparison of the critical buckling load ($\bar{N}_{cr}$) of Al/Al_2O_3 plates (Type A)

γ	*a/b*	*a/h*	**Théorie**	**power - law index** p					
				0	0.5	1	2	5	10
0	0.5	5	present	6.7482	4.5091	3.5203	2.7412	2.2031	1.9419
			HSDT (Nguyen *et al*. 2014)	6.7204	4.4221	3.4164	2.6450	2.1479	1.9210
			TSDT (Thai and Choi 2012)	6.7203	4.4235	3.4164	2.6451	2.1484	1.9213
		10	present	7.4335	4.9084	3.8315	3.0165	2.5043	2.2342
			HSDT (Nguyen *et al*. 2014)	7.4053	4.8190	3.7111	2.8896	2.4163	2.1897
			TSDT (Thai and Choi 2012)	7.4053	4.8206	3.7111	2.8897	2.4165	2.1896
		20	present	7.6104	5.0050	3.9106	3.0930	2.5928	2.3214
			HSDT (Nguyen *et al*. 2014)	7.5993	4.9298	3.7930	2.9581	2.4944	2.2692
			TSDT (Thai and Choi 2012)	7.5993	4.9315	3.7930	2.9582	2.4944	2.2690
	1	5	present	16.0518	10.8051	8.4448	6.5376	5.1456	4.5007
			HSDT (Nguyen *et al*. 2014)	16.0216	10.6215	8.2247	6.3430	5.0513	4.4800
			TSDT (Thai and Choi 2012)	16.0211	10.6254	8.2245	6.3432	5.0531	4.4807
		10	present	18.6639	12.3579	9.6441	7.5712	6.2404	5.5526
			HSDT (Nguyen *et al*. 2014)	18.5786	12.1181	9.3391	7.2630	6.0346	5.4530
			TSDT (Thai and Choi 2012)	18.5785	12.1229	9.3391	7.2631	6.0353	5.4528
		20	present	19.3936	12.7656	9.9715	7.8783	6.5912	5.8969
			HSDT (Nguyen *et al*. 2014)	19.3528	12.5616	9.6675	7.5371	6.3446	5.7674
			TSDT (Thai and Choi 2012)	19.3528	12.5668	9.6675	7.5371	6.3448	5.7668

Table 9 (Continued)

1	0.5	5	present	5.3986	3.6072	2.8162	2.1930	1.7624	1.5535
			HSDT (Nguyen *et al*. 2014)	5.3763	3.5377	2.7331	2.1160	1.7183	1.5368
			TSDT (Thai and Choi 2012)	5.3762	3.5388	2.7331	2.1161	1.7187	1.5370
		10	present	5.9468	3.9267	3.0652	2.4132	2.0034	1.7874
			HSDT (Nguyen *et al*. 2014)	5.9243	3.8552	2.9689	2.3117	1.9330	1.7517
			TSDT (Thai and Choi 2012)	5.9243	3.8565	2.9689	2.3117	1.9332	1.7517
		20	present	6.0883	4.0040	3.1285	2.4744	2.0743	1.8571
			HSDT (Nguyen *et al*. 2014)	6.0794	3.9438	3.0344	2.3665	1.9955	1.8153
			TSDT (Thai and Choi 2012)	6.0794	3.9452	3.0344	2.3665	1.9955	1.8152
	1	5	present	8.0259	5.4025	4.2224	3.2688	2.5728	2.2503
			HSDT (Nguyen *et al*. 2014)	8.0108	5.3108	4.1124	3.1715	2.5256	2.2400
			TSDT (Thai and Choi 2012)	8.0105	5.3127	4.1122	3.1716	2.5265	2.2403
		10	present	9.3319	6.1789	4.8220	3.7856	3.1202	2.7763
			HSDT (Nguyen *et al*. 2014)	9.2893	6.0590	4.6696	3.6315	3.0173	2.7265
			TSDT (Thai and Choi 2012)	9.2893	6.0615	4.6696	3.6315	3.0177	2.7264
		20	present	9.6968	6.3828	4.9857	3.9391	3.2956	2.9484
			HSDT (Nguyen *et al*. 2014)	9.6764	6.2808	4.8337	3.7686	3.1723	2.8837
			TSDT (Thai and Choi 2012)	9.6764	6.2834	4.8337	3.7686	3.1724	2.8834

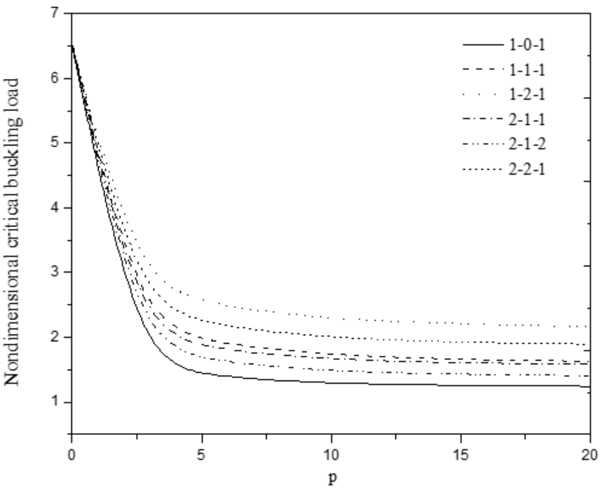

Fig. 6 Effect of the power-law index p on the critical buckling load $(\hat{N}_{cr})$ of Al/Al_2O_3 square sandwich plates ($a/h=10$, Type C).

Table 11Nondimensional critical buckling loads ($\bar{N}_{cr}$) of Al/Al_2O_3 square sandwich plates subjected to biaxial compressive loads ($\gamma = 1$, Type B)

a/h	scheme	*p* 0	0.5	1	5	10
5	**1-1-1**	3.0420	2.6861	2.5170	2.2326	2.1832
	1-2-1	3.4979	2.8840	2.5985	2.1504	2.077
	2-2-1	2.7574	2.4480	2.3000	2.0337	1.9788
10	**1-1-1**	3.3232	2.9675	2.8044	2.5630	2.5324
	1-2-1	3.8448	3.1993	2.9100	2.5229	2.4835
	2-2-1	3.0163	2.7437	2.6255	2.4579	2.4294
100	**1-1-1**	3.3801	3.0522	2.9026	2.6945	2.6740
	1-2-1	3.9095	3.2918	3.0175	2.6763	2.6530
	2-2-1	3.0814	2.8494	2.7525	2.6367	2.6208

From this table, it is found that, for the same sandwich plate scheme, the increase in the power index and aspect ratio a / h increased the critical value of the buckling load.

Figure 6 plots the variation of the critical buckling load versus the power law index and for different scheme of sandwich plate. It has seen a rapid decrease of the critical buckling loads until a value of $p = 5$, Once exceeding this value, the critical buckling loads tends to keep a more or less constant shape and this whatever the sandwich plate used.

4. Conclusions

Bending, buckling and vibration analysis of functionally graded sandwich plate is carried out in the present study by an improved quasi 3D theory. Three different sandwich plates were studied. The results generated in the present work for three cases analyzed namely buckling, bending and free vibration were compared with the results of various theories from the literature. This comparison revealed that the present theory is very precise. A detailed parametric study was presented to highlight the various factors influencing the behavior of sandwich plates.

Based on the Numerical results section of this research, the following considerations are valuable:

The transverse displacement increases as the power law index p increases.

The axial non dimensional stress is tensile at the top surface and compressive at the bottom surface.

The in-plane tangential stress is tensile at the bottom surface and compressive at the top surface of the FG plates.

The distribution of the transverse shear stress through

Table 10 Nondimensional critical buckling loads ($\bar{N}_{cr}$) of Al/Al_2O_3 square sandwich plates subjected to biaxial compressive loads ($\gamma = 1, a/h = 10$, Type C)

p	Theory	1-0-1	2-1-2	2-1-1	1-1-1	2-2-1	1-2-1
0	present	6.53239	6.53239	6.53239	6.53239	6.53239	6.53239
	HSDT (Nguyen *et al*. 2014)	6.50566	6.50566	6.50566	6.50566	6.50566	6.50566
	TSDT (Zenkour 2005b)	6.50248	6.50248	6.50248	6.50248	6.50248	6.50248
	SSDT (Zenkour 2005b)	6.50303	6.50303	6.50303	6.50303	6.50303	6.50303
	HSDT (Neves *et al*. 2012)	6.50266	6.50266	6.50266	6.50266	6.50266	6.50266
	Quasi-3D (Neves *et al*. 2012)	6.47652	6.47652	6.47652	6.47652	6.47652	6.47652
0.5	present	3.77542	4.06891	4.20890	4.31559	4.49937	4.69824
	HSDT (Nguyen *et al*. 2014)	3.67832	3.96760	4.10999	4.21622	4.40304	4.60760
	TSDT (Zenkour 2005b)	3.68219	3.97042	4.11235	4.21823	4.40499	4.60841
	SSDT (Zenkour 2005b)	3.68284	3.97097	4.11269	4.21856	4.40519	4.60835
	HSDT (Neves *et al*. 2012)	3.59354	3.87157	4.00853	4.11071	4.29073	4.48676
	Quasi-3D (Neves *et al*. 2012)	3.58096	3.85809	3.99480	4.09641	4.27592	4.47110
1	present	2.68780	3.03833	3.21593	3.35339	3.59508	3.86818
	HSDT (Nguyen *et al*. 2014)	2.58410	2.92060	3.09759	3.23299	3.47544	3.75403
	TSDT (Zenkour 2005b)	2.58357	2.92003	3.09697	3.23237	3.47472	3.75328
	SSDT (Zenkour 2005b)	2.58423	2.92060	3.09731	3.23270	3.47490	3.75314
	HSDT (Neves *et al*. 2012)	2.53913	2.86503	3.03679	3.16779	3.40280	3.67204
	Quasi-3D (Neves *et al*. 2012)	2.53062	2.85563	3.02733	3.15750	3.39207	3.66013
5	present	1.39547	1.63023	1.81826	1.91731	2.19255	2.50656
	HSDT (Nguyen *et al*. 2014)	1.32948	1.52155	1.70203	1.79002	2.05633	2.36760
	TSDT (Zenkour 2005b)	1.32910	1.52129	1.70176	1.78978	2.05605	2.36734
	SSDT (Zenkour 2005b)	1.33003	1.52203	1.70224	1.79032	2.05644	2.36744
	HSDT (Neves *et al*. 2012)	1.32331	1.50935	1.68594	1.77072	2.03078	2.33036
	Quasi-3D (Neves *et al*. 2012)	1.31829	1.50409	1.68128	1.76507	2.02534	2.32354
10	present	1.28686	1.47198	1.65311	1.71918	1.98553	2.27897
	HSDT (Nguyen *et al*. 2014)	1.24406	1.37341	1.54622	1.59758	1.85403	2.14020
	TSDT (Zenkour 2005b)	1.24363	1.37316	1.54595	1.59736	1.85376	2.13995
	SSDT (Zenkour 2005b)	1.24475	1.37422	1.56721	1.59728	1.57287	2.19087
	HSDT (Neves *et al*. 2012)	1.24090	1.36547	1.53468	1.58421	1.83573	2.10897
	Quasi-3D (Neves *et al*. 2012)	1.23599	1.36044	1.53036	1.57893	1.83083	2.10275

the thickness of the plate is not parabolic except the case of isotropic plate.

The increase in the power index p reduces the frequency.

The increase in the power index and aspect ratio a / h increased the critical value of the buckling load.

The kinematics used in this research can be extended to study other cases of structures such as nano-plates, beams and nano-beams with or without elastic foundation (Bouadi *et al*. (2018), Bellifa *et al*. (2017)).

References

Abdelaziz, H.H., Ait Amar Meziane, M., Bousahla, A.A., Tounsi, A., Mahmoud, S.R. and Alwabli, A.S. (2017), "An efficient hyperbolic shear deformation theory for bending, buckling and free vibration of FGM sandwich plates with various boundary conditions", *Steel Compos. Struct.*, **25**(6), 693-704.

Abdelaziz, H.H., Atmane, H.A., Mechab I., Boumia L, Tounsi, A. and AddaBedia E.A. (2011), "Static analysis of functionally graded sandwich plates using an efficient and simple refined theory", *Chin. J. Aeronaut.,* **24**, 434-448. https://doi.org/10.1016/S1000-9361(11)60051-4.

Ahmed, A. (2014), "Post buckling analysis of sandwich beams with functionally graded faces using a consistent higher order theory", *Int. J. Civil, Struct., Environ*., **4**(2), 59-64.

Ait Amar Meziane, M., Abdelaziz, H.H. and Tounsi, A. (2014), "An efficient and simple refined theory for buckling and free vibration of exponentially graded sandwich plates under various boundary conditions", *J. Sandw. Struct. Mater.,***16**(3), 293-318. https://doi.org/10.1177/1099636214526852.

Ait Sidhoum, I., Boutchicha, D., Benyoucef , S. and Tounsi, A. (2017), "An original HSDT for free vibration analysis of functionally graded plates", *Steel Compos. Struct., Int. J.*, **25**(6), 735-745. https://doi.org/10.12989/scs.2017.25.6.735.

Ait Sidhoum, I., Boutchicha, D., Benyoucef , S. and Tounsi, A., (2018), "A novel quasi-3D hyperbolic shear deformation theory for vibration analysis of simply supported functionally graded plates" . *Smart Structures and Systems,* **22**(3), 303-314.

Akavci, S.S. (2016), "Mechanical behavior of functionally graded sandwich plates on elastic foundation", *Compos. Part B.,* **96**, 136-152. https://doi.org/10.1016/j.compositesb.2016.04.035.

Alipour, M.M. and Shariyat, M. (2014), "Analytical stress analysis of annular FGM sandwich plates with non-uniform shear and normal tractions, employing a zigzag elasticity plate theory", *Aerosp. Sci. Technol.,* **32**(1), 235-259. https://doi.org/10.1016/j.ast.2013.10.007.

Al-shujairi. M, and Çağrı, Mollamahmutoğlu (2018), "Buckling and free vibration analysis of functionally graded sandwich micro-beams resting on elastic foundation by using nonlocal strain gradient theory in conjunction with higher order shear theories under thermal effect", *Composites Part B*, **154**, 292-312. https://doi.org/10.1016/j.compositesb.2018.08.103.

Amnieh, H.B., Zamzam, M.S. and Kolahchi, R. (2018), "Dynamic analysis of non-homogeneous concrete blocks mixed by SiO_2 nanoparticles subjected to blast load experimentally and theoretically", *Construct. Build. Mater.,* **174**, 633-644.

Attia, A., Bousahla, A.A., Tounsi, A., Mahmoud, S.R., Alwabli, A.S. (2018), "A refined four variable plate theory for thermoelastic analysis of FGM plates resting on variable elastic foundations", *Struct. Eng. Mech*., **65**(4), 453-464.

BachirBouiadjra, R., Mahmoudi, A., Benyoucef, S., Tounsi, A. and Bernard, F., (2018), "Analytical investigation of bending response of FGM plate using a new quasi 3D shear deformation theory: Effect of the micromechanical models", *Struct. Eng. Mech*, **66**(3), 317-328. https://doi.org/10.12989/sem.2018.66.3.317.

Bellifa, H., Benrahou, K.H., Bousahla, A.A., Tounsi, A. and Mahmoud, S.R. (2017), "A nonlocal zeroth-order shear deformation theory for nonlinear postbuckling of nanobeams", *Struct. Mech. Eng.*, **62**(6), 695-702. https://doi.org/10.12989/sem.2017.62.6.695.

Bessaim, A., Houari, M.S.A., Tounsi, A., Mahmoud, S.R. and AddaBedia, E.A. (2013), "A new higher-order shear and normal deformation theory for the static and free vibration analysis of sandwich plates with functionally graded isotropic face sheets", *Sandw. Struct. Mater.,* **15**(6), 671-703. https://doi.org/10.1177/1099636213498888.

Bilouei, B.S., Kolahchi, R. and Bidgoli, M.R., (2016), "Buckling of concrete columns retrofitted with Nano-Fiber Reinforced Polymer (NFRP)", *Comput*. *Concrete*, **18**(5), 1053-1063.

Bouadi, A., Bousahla, A.A., Houari, M.S.A., Heireche, H. and Tounsi, A. (2018), "A new nonlocal HSDT for analysis of stability of single layer graphene sheet", *Adv. Nano Res.*, **6**(2), 147-162.

Bouhadra A,.Tounsi A,.Bousahla A.A,.Benyoucef, S. and S.R. Mahmoud, (2018), "Improved HSDT accounting for effect of thickness stretching in advanced composite plates", *Struct. Eng. Mech.,* **66**(1), 61-73.

Bourada, F., Amara, K., Bousahla, A.A., Tounsi, A. and Mahmoud, S.R. (2018), "A novel refined plate theory for stability analysis of hybrid and symmetric S-FGM plates", *Struct. Eng. Mech.,* **68**(6), 661-675.

Bourada, F.,Bousahla, A.A.,Bourada,M., Azzaz, A., Zinata, A. and Tounsi,A. (2019), "Dynamic investigation of porous functionally graded beam using a sinusoidal shear deformation theory", *Wind Struct..,* **28**(1), 19-30.

Bourada, M., Tounsi, A., Houari, M.S.A. and AddaBedia, E.A. (2012), "A new four-variable refined plate theory for thermal buckling analysis of functionally graded sandwich plates", *J. Sandw*. *Struct*. *Mater*.,**14**(1), 5-33. https://doi.org/10.1177/1099636211426386.

Bourada. F., Amara. K. and Tounsi, A. (2016), "Buckling analysis of isotropic and orthotropic plates using a novel four variable refined plate theory", *Steel Compos. Struct*., **21**(6), 1287-1306.

Bousahla, A.A., Benyoucef, S., Tounsi, A. and Mahmoud, S.R. (2016), "On thermal stability of plates with functionally graded coefficient of thermal expansion", *Struct. Eng. Mech*., **60**(2), 313-335.

Carrera E, Brischetto S. and Robaldo, A. (2008), "Variable kinematic model for the analysis of functionally graded material plates", *AIAA J,* **46**(1), 194–203. https://doi.org/10.2514/1.32490.

Ebrahimi, F. and Reza, B.M. (2017), "Hygrothermal effects on vibration characteristics of viscoelastic FG nanobeams based on nonlocal strain gradient theory", *Compos. Struct.*, **159**, 433-444. https://doi.org/10.1016/j.compstruct.2016.09.092.

Fakhar, A. and Kolahchi, R. (2018), "Dynamic buckling of magneto rheological fluid integrated by visco-piezo-GPL reinforced plates" , *J. Mech. Sci.,* **144**, 788-799. https://doi.org/10.1016/j.ijmecsci.2018.06.036

Golabchi, H., Kolahchi, R. and RabaniBidgoli, M. (2018), "Vibration and instability analysis of pipes reinforced by SiO2 nanoparticles considering agglomeration effects", *Comput*. *Concrete*, **21**(4), 431-440.

Gupta, A. and Talha, M. (2017), "Nonlinear flexural and vibration response of geometrically imperfect gradient plates using hyperbolic higher-order shearand normal deformation theory", *Compos. Part. B Eng.,***123**, 241-261. https://doi.org/10.1016/j.compositesb.2017.05.010.

Hadji, L, Atmane, H.A., Tounsi, A., Mechab, I. and AddaBedia, E.A., (2011), "Free vibration of functionally graded sandwich plates using four variable refined plate theory", *Appl. Math. Mech.,* **32**, 925-942. https://doi.org/10.1007/s10483-011-1470-9.

Hajmohammad, M.H., Farrokhian, A. and Kolahchi, R. (2018a), "Smart control and vibration of viscoelastic actuator-multiphase nanocomposite conical shells-sensor considering hygrothermal load based on layerwise theory", *Aerosp.Sci*. *Technol*., **78**, 260-270. https://doi.org/10.1016/j.ast.2018.04.030.

Hajmohammad, M.H., Maleki, M. and Kolahchi, R. (2018b), "Seismic response of underwater concrete pipes conveying fluid covered with nano-fiber reinforced polymer layer", *Soil Dyn*. *Earthq*. *Eng*., **110**, 18-27. https://doi.org/10.1016/j.soildyn.2018.04.002.

Hajmohammad, M.H., Zarei, M.S., Nouri, A. and Kolahchi, R. (2017), "Dynamic buckling of sensor/functionally gradedcarbon nanotube-reinforced laminated plates/actuator based on sinusoidal-visco-piezoelasticity theories", *J. Sandw. Struct. Mater.*, https://doi.org/10.1177/1099636217720373.

Hamidi, A., Houari, M.S.A., Mahmoud, S.R. and Tounsi, A., (2015), "A sinusoidal plate theory with 5-unknowns and stretching effect for thermomechanical bending of functionally graded sandwich plates", *Steel Compos. Struct*.,**18**(1), 235-253.

Hebali, H., Tounsi, A., Houari, M.S.A., Bessaim, A. and AddaBedia, E.A. (2014), "New quasi-3D hyperbolic shear deformation theory for the static and free vibration analysis of functionally graded plates", *J. Eng. Mech., ASCE*, **140**, 374-383.

Hosseini, H. and Kolahchi, R. (2018), "Seismic response of functionally graded-carbon nanotubes-reinforced submerged viscoelastic cylindrical shell in hygrothermal environment", *Physica E*, **102**,101-109. https://doi.org/10.1016/j.physe.2018.04.037.

Houari, M.S.A., Benyoucef, S., Mechab, I., Tounsi, A and Adda Bedia, E.A. (2011), "Two variable refined plate theory for thermoelastic bending analysis of functionally graded sandwich plates", *J. Therm. Stresses,* **34**(4), 315-334. https://doi.org/10.1080/01495739.2010.550806.

Karami, B. and Janghorban, M. (2019), "On the dynamics of porous nanotubes with variable material properties and variable thickness", *J. Eng. Sci.,* **136**(C), 53-

66. https://doi.org/10.1016/j.ijengsci.2019.01.002.

Karami, B., Janghorban, M. and Li, L. (2018a), "On guided wave propagation in fully clamped porous functionally graded nanoplates", *Acta Astronaut.,* **143**, 380-390. https://doi.org/10.1016/j.actaastro.2017.12.011.

Karami, B., Janghorban, M., Shahsavari, D. and Tounsi, A, (2018h), "A size-dependent quasi-3D model for wave dispersion analysis of FG nanoplates", *Steel Compos. Struct.,* **28**(1), 99-110. https://doi.org/10.12989/scs.2018.28.1.099.

Karami, B., Janghorban, M. and Tounsi, A. (2018e), "Variational approach for wave dispersion in anisotropic doubly-curved nanoshells based on a new nonlocal strain gradient higher order shell theory", *Thin-Walled Struct,***129**, 251–264. https://doi.org/10.1016/j.tws.2018.02.025.

Karami, B., Janghorban, M. and Tounsi, A. (2018g), "Nonlocal strain gradient 3d elasticity theory for anisotropic spherical nanoparticles", *Steel Compos. Struct,* **27**(2), 201-216.

Karami, B., Shahsavari, D., Janghorban, M., Dimitri, R. and Tornabene, F. (2019), "Wave Propagation of Porous Nanoshells", *Nanomaterials*, **9**(1), 1-19. https://doi.org/10.3390/nano9010022.

Karami, B., Shahsavari, D., Li, L., Karami, M. and Janghorban, M. (2018c), "Thermal buckling of embedded sandwich piezoelectric nanoplates with functionally graded core by a nonlocal second-order shear deformation theory", *Proceedings of the Institution of Mechanical Engineers, Part C*, **233**(1), 287-301.

Karami, B., Shahsavari, D., Nazemosadat, S.M.R., Li, L. (2018d), "Thermal buckling of smart porous functionally graded nanobeam rested on kerr foundation", *Steel Compos. Struct.,* **29**(3), 349-362. https://doi.org/10.12989/scs.2018.29.3.349.

Karami, B., Janghorban, M. and Tounsi. A. (2018f), "Galerkin's approach for buckling analysis of functionally graded anisotropic nanoplates/different boundary conditions", *Eng. Comput.*, 1-20. https://doi.org/10.1007/s00366-018-0664-9.

Karami, B., Shahsavari, D. and Li, L. (2018b), "Temperature-dependent flexural wave propagation in nanoplate-type porous heterogenous material subjected to in-plane magnetic field", *J. Therm. Stresses*, **41**(4), 483-499. https://doi.org/10.1080/01495739.2017.1393781.

Kolahchi, R. (2017), "A comparative study on the bending, vibration and buckling of viscoelastic sandwich nano-plates based on different nonlocal theories using DC, HDQ and DQ methods", *Aerosp. Sci. Technol.*, **66**, 235-248. https://doi.org/10.1016/j.ast.2017.03.016.

Kolahchi, R. and Cheraghbak, A. (2017), "Agglomeration effects on the dynamic buckling of viscoelastic microplates reinforced with SWCNTs using Bolotin method", *Nonlin.Dyn.*, **90**(1), 479492. https://doi.org/10.1007/s11071-017-3676-x.

Kolahchi, R. and Arani, A.J. (2016), "Buckling analysis of embedded concrete columns armed with carbon nanotubes", *Comput. Concrete,* **17**(5), 567-578.

Kolahchi, R., Keshtegar, B. and Fakhar, M.H. (2017b), "Optimization of dynamic buckling for sandwich nanocomposite plates with sensor and actuator layer based on sinusoidal-visco-piezoelasticity theories using Grey Wolf algorithm", *J. Sandw. Struct. Mater*. https://doi.org/10.1177/1099636217731071.

Kolahchi, R., Zarei, M.S., Hajmohammad, M.H. and Nouri, A. (2017a), "Wave propagation of embedded viscoelastic FG-CNT-reinforced sandwich plates integrated with sensor and actuator based on refined zigzag theory", *J. Mech. Sci.*, **130**, 534-545. https://doi.org/10.1016/j.ijmecsci.2017.06.039.

Kolahchi, R., Safari, M. and Esmailpour, M. (2016), "Dynamic stability analysis of temperature-dependent functionally graded CNT-reinforced visco-plates resting on orthotropic elastomeric medium", *Compos. Struct.,***150**, 255-265. https://doi.org/10.1016/j.compstruct.2016.05.023.

Li, D., Deng, Z. and Xiao, H. (2016), "Thermomechanical bending analysis of functionally graded sandwich plates using four-variable refined plate theory", *Compos. Pt B.,* **106**, 107-119. https://doi.org/10.1016/j.compositesb.2016.08.041.

Li, X.F. (2008), "A unified approach for analyzing static and dynamic behaviors of functionally graded Timoshenko and Euler-Bernoulli beams", *J. Sound Vib..,* **318**, 1210-1229. https://doi.org/10.1016/j.jsv.2008.04.056.

Madani, H., Hosseini, H. and Shokravi, M. (2016), "Differential cubature method for vibration analysis of embedded FG-CNT reinforced piezoelectric cylindrical shells subjected to uniform and non-uniform temperature distributions", *Steel Compos. Struct*., **22**(4), 889-913.

Mahmoudi, A., Benyoucef, S., Tounsi, A., Benachour, A., AddaBedia, E.A and Mahmoud, S.R. (2017), "A refined quasi-3D shear deformation theory for thermo-mechanical behaviour of functionally graded sandwich plates on elastic foundations", *J. Sandw. Struct. Mater.,* https://doi.org/10.1177/1099636217727577.

Mahmoudi, A., Benyoucef, S., Tounsi, A., Benachour, A and Adda Bedia, E.A. (2018), "On the effect of the micromechanical models on the free vibration of rectangular FGM plate resting on elastic foundation", *Struct. Eng. Mech.*, **14**(2), 117-128. https://doi.org/10.12989/eas.2018.14.2.117.

Mantari, J.L., Oktem, A.S. and Soares, O.G. (2012), "Bending response of functionally graded plates by using a new higher order shear deformation theory", *Compos Struct.,* **94**, 714-723. https://doi.org/10.1016/j.compstruct.2011.09.007.

Mantari, J.L. and Soares, C.G. (2014), "A trigonometric plate theory with 5-unknowns and stretching effect for advanced composite plates", *Compos. Struct*., **107**, 396-405. https://doi.org/10.1016/j.compstruct.2013.07.046.

Meksi, A., Benyoucef, S., Houari, M.S.A. and Tounsi, A. (2015), "A simple shear deformation theory based on neutral surface position for functionally graded plates resting on Pasternak elastic foundations", *Struct. Eng. Mech*., **53**(6), 1215-1240.

Meksi, R, Benyoucef, S., Mahmoudi, A., Tounsi, A., Adda Bedia, E.A. and Mahmoud, S.R. (2019), "An analytical solution for bending, buckling and vibration responses of FGM sandwich plates", *J. Sandw. Struct. Mater*., **21**(2), 727-757. https://doi.org/10.1177/1099636217698443.

Menasria, A., Bouhadra, A., Tounsi, A., Bousahla, A.A. and S.R. Mahmoud (2017), "A new and simple HSDT for thermal stability analysis of FG sandwich plates". *Steel Compos.Struct*., **25**(2), 157-175. https://doi.org/10.12989/scs.2017.25.2.157.

Merdaci, S., Tounsi, A., Houari, M.S.A., Mechab, I., Hebali, H., Benyoucef, S. (2011), "Two new refined shear displacement models for functionally graded sandwich plates". *Arch. Appl. Mech*., **81**, 1507–1522. https://doi.org/10.1007/s00419-010-0497-5.

Mindlin, R.D. (1951), "Influence of rotary inertia and shear on flexural motions of isotropic elastic plates", *J. Appl. Mech.,* **18**, 31-38.

Natarajan, S. and Manickam, G. (2012), "Bending and vibration of functionally graded material sandwich plates using an accurate theory", *Finite. Elem. Anal. Des*., **57**, 32-42. https://doi.org/10.1016/j.finel.2012.03.006.

Neves, A., Ferreira, A., Carrera, E., Cinefra, M., Jorge, R. and Soares, C. (2012), "Buckling analysis of sandwich plates with functionally graded skins using a new quasi-3D hyperbolic sine shear deformation theory and collocation with radial basis functions", *J. Appl. Math. Mech*., **92**(9), 749-766. https://doi.org/10.1002/zamm.201100186.

Neves, A.M.A., Ferreira, A.J.M., Carrera, E., Cinefra, M., Roque, C.M.C., Jorge, R.M.N and Soares, C.M.M. (2013), "Static, free vibration and buckling analysis of isotropic and sandwich functionally graded plates using a quasi-3D higher-order shear deformation theory and a meshless technique", *Compos Part B: Eng.,* **44**, 657-674. https://doi.org/10.1016/j.compositesb.2012.01.089.

Nguyen, V.H., Nguyen, T.K., Thai, H.T. and Vo, T.P. (2014), "A new inverse trigonometric shear deformation theory for isotropic and functionally graded sandwich plates", *Compos. Pt. B Eng.,* **66**, 233-246. https://doi.org/10.1016/j.compositesb.2014.05.012.

Petrov, N.A., Gorbatikh, L. and Lomov, V.S. (2018), "A parametric study assessing performance of eXtended Finite Element Method in application to the cracking process in cross-ply composite laminates", *Compos. Struct.,***187**, 498-508. https://doi.org/10.1016/j.compstruct.2017.12.014.

Reissner, E. (1945), "The effect of transverse shear deformation on the bending of elastic plates", *J. Appl. Mech*., **12**(2), 69-77.

Sekkal, M., Fahsi, B., Tounsi, A. and Mahmoud, S.R. (2017), "A novel and simple higher order shear deformation theory for stability and vibration of functionally graded sandwich plate", *Steel Compos. Struct.,* **25**(4), 389-401.

Shahsavari, D., Karami, B., Fahham, H.R. and Li, L. (2018c), "On the shear buckling of porous nanoplates using a new size-dependent quasi-3d shear deformation theory", *Acta Mech.***229**(11), 4549-4573. https://doi.org/10.1007/s00707-018-2247-7.

Shahsavari, D., Karami, B., Janghorban, M. and Li, L. (2017), "Dynamic characteristics of viscoelastic nanoplates under moving load embedded within visco-Pasternak substrate and hygrothermal environment", *Mater. Res. Exp.,***4**(8), 085013.

Shahsavari, D., Karami, B., Janghorban, M. and Li, L. (2018a), "Damped vibration of a graphene sheet using a higher-order nonlocal strain-gradient Kirchhoff plate model", *Comptes Rendus Mécanique,* **346** (12), 1216-1232. https://doi.org/10.1016/j.crme.2018.08.011.

Shahsavari, D., Shahsavari, M., Li, L. and Karami, B. (2018b), "A novel quasi-3D hyperbolic theory for free vibration of FG plates with porosities resting on Winkler/Pasternak/Kerr foundation", *Aerospace Science and Technology*, **72**, 134-149. https://doi.org/10.1016/j.ast.2017.11.004.

She, G.L., Yuan, F.G., Ren, R.Y. and Xiao, W.S. (2017), "On buckling and postbuckling behavior of nanotubes", *J. Eng. Sci.,* **121**, 130-142. https://doi.org/10.1016/j.ijengsci.2017.09.005.

She, G.L., Yuan, F.G., Karami, B., Ren, Y.R. and Xiao, W.S. (2019), "On nonlinear bending behavior of fg porous curved nanotubes", *Int. J. Eng. Sci.,* **135**, 58-74. https://doi.org/10.1016/j.ijengsci.2018.11.005.

She, G.L., Yuan, F.G. and Ren, Y.R. (2018), "On wave propagation of porous nanotubes", *Int. J. Eng. Sci*, **130**, 62-74. https://doi.org/10.1016/j.ijengsci.2018.05.002.

Taibi, F.Z, Benyoucef, S., Tounsi, A., BachirBouiadjra, R., AddaBedia, E.A. and Mahmoud, S.R. (2015), "A simple shear deformation theory for thermo-mechanical behaviour of functionally graded sandwich plates on elastic foundations", *J. Sandw. Struct. Mater.*, **17**(2), 99-129. https://doi.org/10.1177/1099636214554904.

Thai, H.T. and Kim, S.E. (2013), "A simple higher-order shear deformation theory for bending and free vibration analysis of functionally graded plates", *Compos. Struct.,* **96**, 165-173. https://doi.org/10.1016/j.compstruct.2012.08.025.

Thai, H.T. and Choi, D.H. (2013), "A simple first-order shear deformation theory for the bending and free vibration analysis of functionally graded plates", *Compos. Struct*., **101**, 332-340. https://doi.org/10.1016/j.compstruct.2013 .02.019.

Thai, H.T. and Choi, D.H. (2012), "An efficient and simple refined theory for buckling analysis of functionally graded plates", *Appl. Math. Model*., **36**, 1008-1022. https://doi.org/10.1016/j.apm.2011.07.062

Thai, H.T., Nguyen, T.K. and Vo, T. (2014), "Analysis of functionally graded sandwich plates using a new first- order shear deformation theory", *Europ. J. Mech. A/Solids.,* **45**, 211-225. https://doi.org/10.1016/j.euromechsol.2013.12.008.

Tounsi, A., Houari, M.S.A. and Benyoucef, S. (2013), "A refined trigonometric shear deformation theory for thermoelastic bending of functionally graded sandwich plates", *Aerosp. Sci. Technol.*, **24**(1), 209-220. https://doi.org/10.1016/j.ast.2011.11.009.

Uymaz, B. and Aydogdu, M. (2007), "Three-dimensional vibration analyses of functionally graded plates under various boundary conditions"*, J. Reinf. Plast. Compos.,* **26**(18), 1847-1863. https://doi.org/10.1177/0731684407081351.

Wu, C.P. and Chiu, K.H. (2011), "RMVT-based meshless collocation and element-free Galerkin methods for the quasi-3D free vibration analysis of multilayered composite and FGM plates", *Compos. Struct.* **93**(5), 1433-1448. https://doi.org/10.1016/j.compstruct.2010.11.015.

Xiang, S., Jin, Y., Bi, Z., Jiang, S. and Yang, M. (2011), "A n-order shear deformation theory for free vibration of functionally graded and composite sandwich plates", *Compos. Struct*., **93**, 2826-2832. https://doi.org/10.1016/j.compstruct.2011.05.022.

Xiang, S., Kang, G., Yang, M. and Zhao, Y. (2013), "Natural frequencies of sandwich plate with functionally graded face and homogeneous core", *Compos. Struct*., **96**, 226-231. https://doi.org/10.1016/j.compstruct.2012.09.003.

Zamanian, M., Kolahchi, R. and Bidgoli, M.R. (2017), "Agglomeration effects on the buckling behaviour of embedded concrete columns reinforced with SiO2 nano-particles", *Wind Struct*., **24**(1), 43-57. https://doi.org/10.12989/was.2017.24.1.043.

Zarei, M.S., Kolahchi, R., Hajmohammad, M.H. and Maleki, M. (2017), "Seismic response of underwater fluid-conveying concrete pipes reinforced with SiO nanoparticles and fiber reinforced polymer (FRP) layer", *Soil Dyn. Earthq. Eng.*, **103**, 76-85. https://doi.org/10.1016/j.soildyn.2017.09.009.

Zenkour, A.M. (2006), "Generalized shear deformation theory for bending analysis of functionally graded materials", *Appl Math Model*, **30**, 67-84. https://doi.org/10.1016/j.apm.2005.03.009.

Zenkour, M. (2013), "Bending analysis of functionally graded sandwich plates using a simple four-unknown shear and normal deformations theory", *J. Sandwich. Struct. Mater*., **15**, 629-656. https://doi.org/10.1177/1099636213498886.

Zenkour, A.M. (2005a), "A comprehensive analysis of functionally graded sandwich plates: Part 1-Deflection and stresses", *Inter. J. Sol. Struct*., **42**, 5224-5242. https://doi.org/10.1016/j.ijsolstr.2005.02.015.

Zenkour, A.M. (2005b), "A Comprehensive Analysis of Functionally Graded Sandwich Plates: Part 2—Buckling and Free Vibration", *Inter. J. of Sol. and Struct*., **42**, 5243-5258. https://doi.org/10.1016/j.ijsolstr.2005.02.016.

Zenkour, A.M. and Alghamdi, N.A. (2010), "Bending analysis of functionally graded sandwich plates under the effect of mechanical and thermal loads", *Mec. Ad. Mater. Struct*., **17**, 419-432. https://doi.org/10.1080/15376494.2010.483323.

CC